AD-A058 362 SINGER CO FAIRFIELD NJ KEARFOTT DIV F/G 14/2
ANGULAR RATE SENSOR PROGRAM.(U)
DEC 77 J L EVANS, R E WEBER DNA001-77-C-0140
UNCLASSIFIED Y259A061 DNA-4529F NL

1 OF 1
AD
A058 382

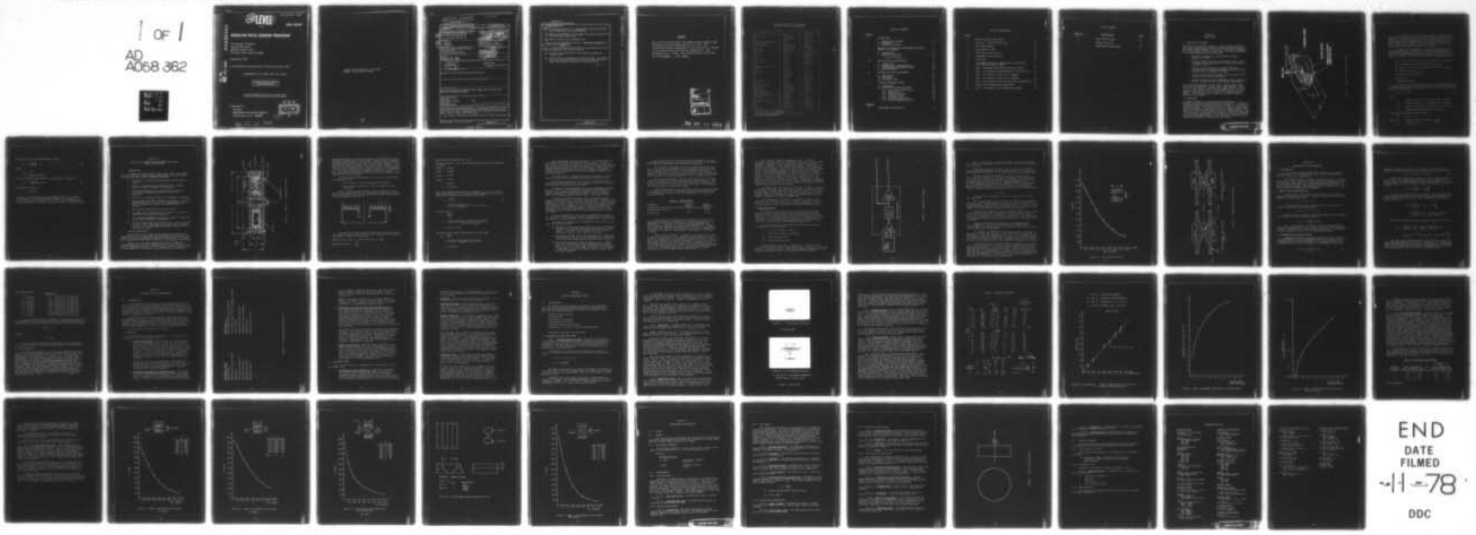

END
DATE
FILMED
-11-78
DDC

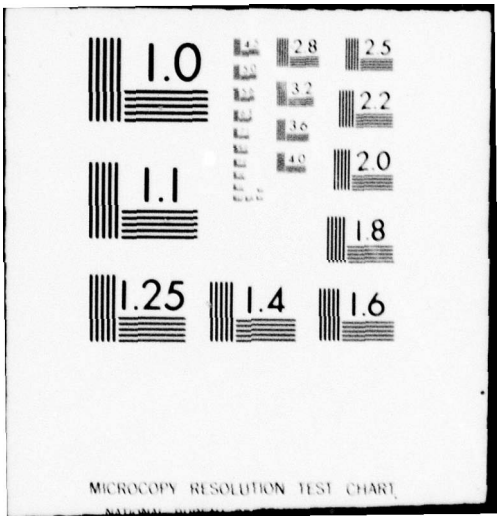
1.0
1.1
1.25
1.4
1.6
1.8
2.0
2.2
2.5
2.8
3.2
3.6
4.0
MICROCOPY RESOLUTION TEST CHART

(12) LEVEL II

SC

DNA 4529F

ANGULAR RATE SENSOR PROGRAM

The Singer Company
Kearfott Division
90 New Dutch Lane
Fairfield, New Jersey 07006

December 1977

Final Report for Period April 1977—December 1977

CONTRACT No. DNA 001-77-C-0140

APPROVED FOR PUBLIC RELEASE;
DISTRIBUTION UNLIMITED.

THIS WORK SPONSORED BY THE DEFENSE NUCLEAR AGENCY
UNDER RDT&E RMSS CODE B344077462 H11CAXSX35275 H2590D.

Prepared for
Director
DEFENSE NUCLEAR AGENCY
Washington, D. C. 20305

Destroy this report when it is no longer needed. Do not return to sender.

(18) DNA, SBIE

62710H

UNCLASSIFIED

SECURITY CLASSIFICATION OF THIS PAGE (When Data Entered)

(19) **REPORT DOCUMENTATION PAGE**

READ INSTRUCTIONS BEFORE COMPLETING FORM

1. REPORT NUMBER: DNA 4529F; AD-E300 298	2. GOVT ACCESSION NO. / 3. RECIPIENT'S CATALOG NUMBER
4. TITLE (and Subtitle): (6) ANGULAR RATE SENSOR PROGRAM	5. TYPE OF REPORT & PERIOD COVERED: (9) Final Report for Period April 1977—December 1977
	6. PERFORMING ORG. REPORT NUMBER: (14) Y259A061
7. AUTHOR(s): (10) J. L. Evans, R. E. Weber	8. CONTRACT OR GRANT NUMBER(s): (15) DNA 001-77-C-0140
9. PERFORMING ORGANIZATION NAME AND ADDRESS: The Singer Company, Kearfott Division, 90 New Dutch Lane, Fairfield, New Jersey 07006	10. PROGRAM ELEMENT, PROJECT, TASK AREA & WORK UNIT NUMBERS: (17) NWET Subtask (16) H11CAXSX352-75
11. CONTROLLING OFFICE NAME AND ADDRESS: Director, Defense Nuclear Agency, Washington, D.C. 20305	12. REPORT DATE: (11) December 1977
	13. NUMBER OF PAGES: 54
14. MONITORING AGENCY NAME & ADDRESS (if different from Controlling Office): (12) 53p.	15. SECURITY CLASS (of this report): UNCLASSIFIED
	15a. DECLASSIFICATION/DOWNGRADING SCHEDULE

16. DISTRIBUTION STATEMENT (of this Report)

Approved for public release; distribution unlimited.

17. DISTRIBUTION STATEMENT (of the abstract entered in Block 20, if different from Report)

18. SUPPLEMENTARY NOTES

This work sponsored by the Defense Nuclear Agency under RDT&E RMSS Code B344077462 H11CAXSX35275 H2590D.

19. KEY WORDS (Continue on reverse side if necessary and identify by block number)

Angular Rate Sensor
High Rates
High Shock Environment
Lower-Power
Wide Dynamic Range

The purpose of this project

20. ABSTRACT (Continue on reverse side if necessary and identify by block number)

This project was a multiphased program. Its purpose was to evaluate the technology associated with the Kearfott Angular Rate Sensor (KARS) and to verify that it was at a level of development such that a production version could be begun. The four phases of the effort were:

(1) Analysis of operational requirements and their impact on the design,

DD FORM 1 JAN 73 1473 EDITION OF 1 NOV 65 IS OBSOLETE

UNCLASSIFIED

SECURITY CLASSIFICATION OF THIS PAGE (When Data Entered)

410 165

1B

20. ABSTRACT (Continued)

(2) Perform design analysis for a design chosen to satisfy the specific set of requirements arrived at ~~in Phase 1~~,

(3) Define test requirements and data reduction techniques appropriate to the design and the application, and

(4) Perform various critical subassembly tests.

These steps were completed satisfactorily. ~~Among other things~~, the following major tasks were also completed:

~~1.~~ A configuration of the KARS satisfying the requirements as set forth by DNA was analyzed and found to be satisfactory.

~~2.~~ A test program was defined and a data reduction technique was analyzed, and

~~3.~~ Various critical subassemblies were built and tested. The results of these tests verified the ability of the design to meet the environmental and performance requirements in the specification.

PREFACE

This work was sponsored by the Defense Nuclear Agency under Government Contract Number DNA 001-77-C-0140. The Contracting Officers Representative for work was T.E. Kennedy of the Shock Physics Directorate, Headquarters, DNA Washington, D.C. 20305. The authorization for this work was DNA H11CXAS, Task X352.

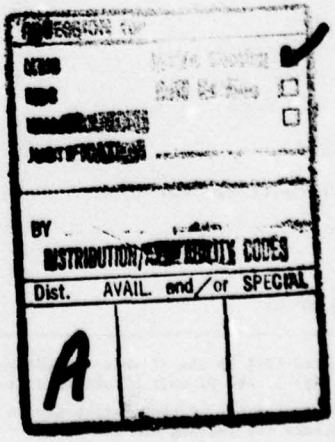

Conversion factors for U.S. customary to metric (SI) units of measurement.

To Convert From	To	Multiply By
angstrom	meters (m)	1.000 000 X E -10
atmosphere (normal)	kilo pascal (kPa)	1.013 25 X E +2
bar	kilo pascal (kPa)	1.000 000 X E +2
barn	meter^2 (m^2)	1.000 000 X E -28
British thermal unit (thermochemical)	joule (J)	1.054 350 X E +3
calorie (thermochemical)	joule (J)	4.184 000
cal (thermochemical)/cm^2	mega joule/m^2 (MJ/m^2)	4.184 000 X E -2
curie	giga becquerel (GBq)*	3.700 000 X E +1
degree (angle)	radian (rad)	1.745 329 X E -2
degree Fahrenheit	degree kelvin (K)	$t_k = (t° f + 459.67)/1.8$
electron volt	joule (J)	1.602 19 X E -19
erg	joule (J)	1.000 000 X E -7
erg/second	watt (W)	1.000 000 X E -7
foot	meter (m)	3.048 000 X E -1
foot-pound-force	joule (J)	1.355 818
gallon (U.S. liquid)	meter^3 (m^3)	3.785 412 X E -3
inch	meter (m)	2.540 000 X E -2
jerk	joule (J)	1.000 000 X E +9
joule/kilogram (J/kg) (radiation dose absorbed)	Gray (Gy)**	1.000 000
kilotons	terajoules	4.183
kip (1000 lbf)	newton (N)	4.448 222 X E +3
kip/inch^2 (ksi)	kilo pascal (kPa)	6.894 757 X E +3
ktap	newton-second/m^2 ($N-s/m^2$)	1.000 000 X E +2
micron	meter (m)	1.000 000 X E -6
mil	meter (m)	2.540 000 X E -5
mile (international)	meter (m)	1.609 344 X E +3
ounce	kilogram (kg)	2.834 952 X E -2
pound-force (lbf avoirdupois)	newton (N)	4.448 222
pound-force inch	newton-meter (N·m)	1.129 848 X E -1
pound-force/inch	newton/meter (N/m)	1.751 268 X E +2
pound-force/foot^2	kilo pascal (kPa)	4.788 026 X E -2
pound-force/inch^2 (psi)	kilo pascal (kPa)	6.894 757
pound-mass (lbm avoirdupois)	kilogram (kg)	4.535 924 X E -1
pound-mass-foot^2 (moment of inertia)	kilogram-meter^2 ($kg·m^2$)	4.214 011 X E -2
pound-mass/foot^3	kilogram/meter^3 (kg/m^3)	1.601 846 X E +1
rad (radiation dose absorbed)	Gray (Gy)**	1.000 000 X E -2
roentgen	coulomb/kilogram (C/kg)	2.579 760 X E -4
shake	second (s)	1.000 000 X E -8
slug	kilogram (kg)	1.459 390 X E +1
torr (mm Hg, 0° C)	kilo pascal (kPa)	1.333 22 X E -1

*The becquerel (Bq) is the SI unit of radioactivity; 1 Bq = 1 event/s.
**The Gray (Gy) is the SI unit of absorbed radiation.

A more complete listing of conversions may be found in "Metric Practice Guide E 380-74," American Society for Testing and Materials.

TABLE OF CONTENTS

LIST OF ILLUSTRATIONS

LIST OF TABLES

SECTION I
INTRODUCTION

1. DESCRIPTION OF REPORT

This report is the final report on a contract whose objective was to determine what was needed to bring the Kearfott Angular Rate Sensor (KARS) design to a state of readiness for production for use by various DNA field contractors. The tasks considered in the performance of this contract were:

1. Analyze the operational requirements and their impact on the KARS.

2. Perform a design analysis on the KARS to make it meet the operational requirements of the specific mission analyzed in Task 1.

3. Outline a test program that provides reasonable assurance that a successful component will also satisfy the operational requirements of DNA.

4. Define a data reduction scheme that optimizes the usefullness of the KARS output data.

5. Perform certain critical subassembly tests required to define the KARS ability to satisfy DNA requirements.

In the following sections of the report, each of the 5 Tasks above will be addressed. Tasks 1 and 2 were combined. Both cover the same material from different viewpoints so no detail is lost. The output of Task 1 was intended to be a draft of a product specification (it is included as an appendix to this Report). The remaining three items are covered as separate sections of the report.

2. BACKGROUND

The KARS is basically a damped angular accelerometer. Its physical character is shown pictorially in Figure 1. It comprises a conductive liquid annulus (mercury) positioned in the gap of a permanent magnet. The conductive liquid is held in a disk-shaped insulating housing. Upon application of an angular input to the case, the liquid annulus initially tends to remain immobile. The relative motion of the liquid to the case is sensed by measurement of the potential generated in the liquid as it cuts the lines of force of the permanent magnet. The potential is measured on two electrodes submerged in the mercury (not shown).

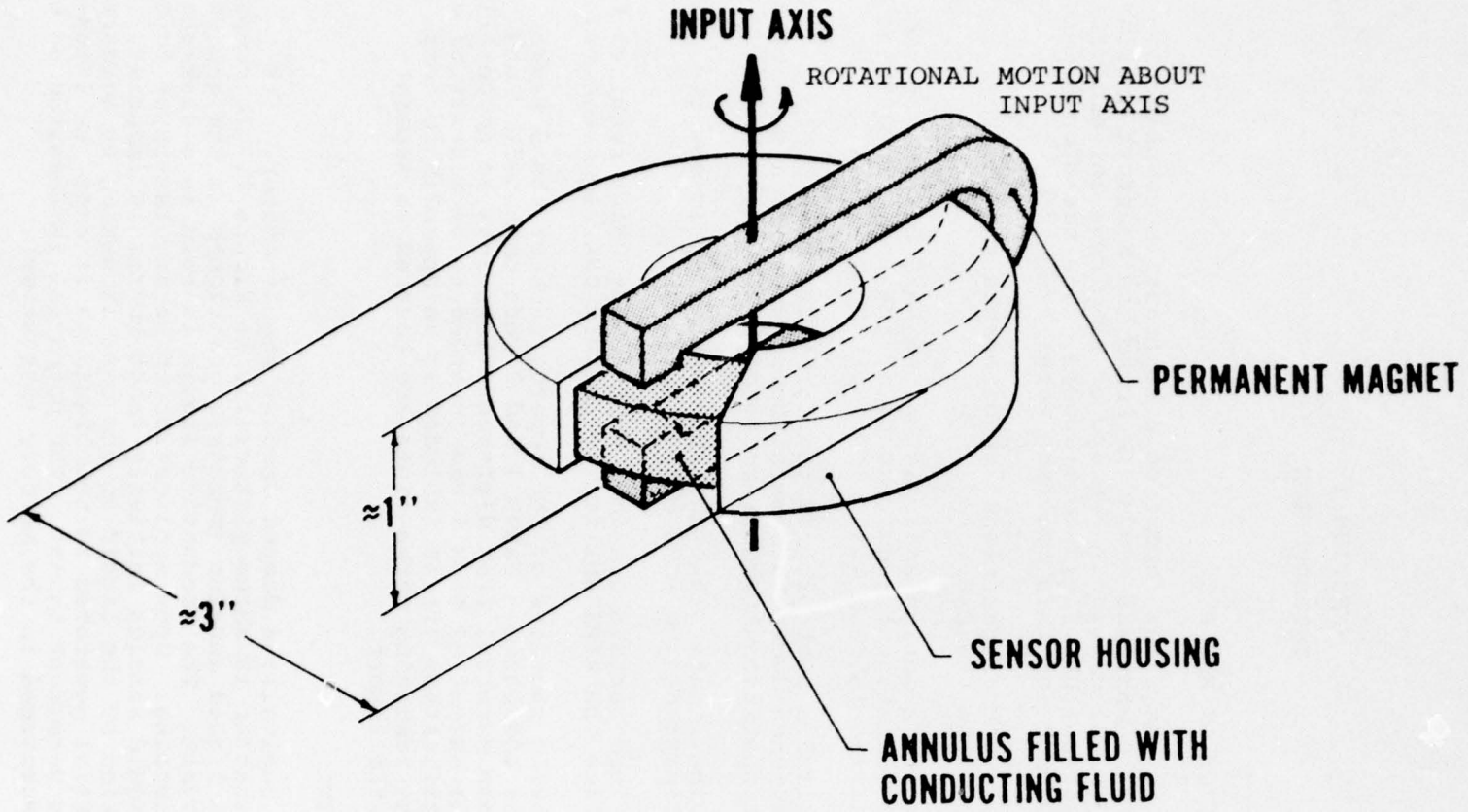

Figure 1. Kearfott Angular Rate Sensor

It is interesting to note that the device is totally self generating in terms of output. No power source is required in its function. The energy used in generating output potential is derived solely from the sensor motion. An amplifier is used for signal enhancement to improve the signal-to-noise ratio of the device in the low-rate region; and, when buffering is desired, to permit mixing of signals in the control system.

The KARS is an unconventional inertial sensor designed to provide dynamic rate information. Its primary advantages over conventional instruments derive from the fact that it has no spinning wheel assembly to wear out and requires no active voltage source to operate. A listing of its specific advantages follows:

- Zero reaction time in the normal MIL-Spec environments
- No temperature sensitivity error coefficient
- Capable of sustaining high shock loads with no damage
- Minimal power dissipation
- Very long operating life
- Low cost.

3. OPERATING PRINCIPLE

The conductive liquid ring used in the KARS assembly acts as a lumped inertia element viscously linked to the instrument housing. The differential equation describing the motion of such a system is given in the following:

$$I\ddot{\theta}_\ell + D\dot{\theta}_\ell = D\dot{\theta}_C \qquad (1)$$

where:

θ_ℓ = Angular response of the liquid ring (radians)

θ_C = Angular input to the instrument case (radians)

I = Moment of inertia of the liquid ring (dyne cm s^2)

D = Viscous damping coefficient (dyne/cm/s).

The equation governing output voltage is:

$$e_o = K\,(\dot{\theta}_C - \dot{\theta}_\ell) \qquad (2)$$

where k = Magnetic generator constant $\left(\frac{V/s}{rad}\right)$

e_o = Output voltage

Solving for e_o in the Laplace domain yields:

$$e_o = \frac{k\ \ddot{\theta}_c(s)}{S + \omega_o} \tag{3}$$

where:

ω_o = D/I

S = Laplace operator

For the frequency domain where $S > j\ \omega_o$, Equation 3 reduces to:

$$e_o = \frac{k\ \ddot{\theta}_c(s)}{S} \approx k\ \dot{\theta}_c(s) \tag{4}$$

Similarly where $S < j\ \omega_o$:

$$e_o = \frac{k}{\omega_o}\ \ddot{\theta}_c(s) \tag{5}$$

It is seen from Equation 4 that the output voltage is a measure of input rate in the higher frequency domain (i.e., where $\omega_o j < s$). On this basis, it is desirable for (ω_o) the corner frequency to be as low as possible and thereby broaden the range of rate measurement.

SECTION II

ANALYSIS OF OPERATIONAL REQUIREMENTS AND THEIR IMPACT ON THE DESIGN

4. INTRODUCTION

The KARS application under study in this effort has several features that have a major impact on the design. They are listed here and discussed in detail item-by-item below:

1. Survival of a 10,000-g 3-millisecond half-sine shock is required.

2. Survival of exposure to a temperature soak anywhere between -29 and +71 degree C is required.

3. Operating temperature will be relatively constant so that dynamic temperature conditions need not be considered.

4. Survival of a MIL Spec vibration environment is required.

5. Two different performance regimes are required. The chief distinguishing factor is that the maximum input rate is either 10 deg/sec in regime A or 30,000 deg/sec in regime B.

6. The required resolution is 2% of full scale.

7. The KARS output is not used in real time. It can be recorded and processed when convenient.

8. The required bandwidth is 500 Hz for regime A; 5000 Hz desired, 2000 Hz required for regime B.

9. The scale factor is to be such that full scale is 5 volts in either case. Many other requirements exist; however, they are of a routine engineering nature and need not be discussed in detail.

5. DETAILED DISCUSSION

The survival of a 10,000-g shock determines the mechanical configuration of the KARS. When the acceleration vector lies in the plane of the ring it produces a peak hydrostatic head of 15,000 psi. The mechanical structure must be capable of restraining this pressure.

Figure 2 is a section through a design of the KARS that analytically meets this shock requirement. The basic concept is to make the KARS sensor out of a strong insulator such as a plastic that is also compatible with mercury. This eliminates any electrical

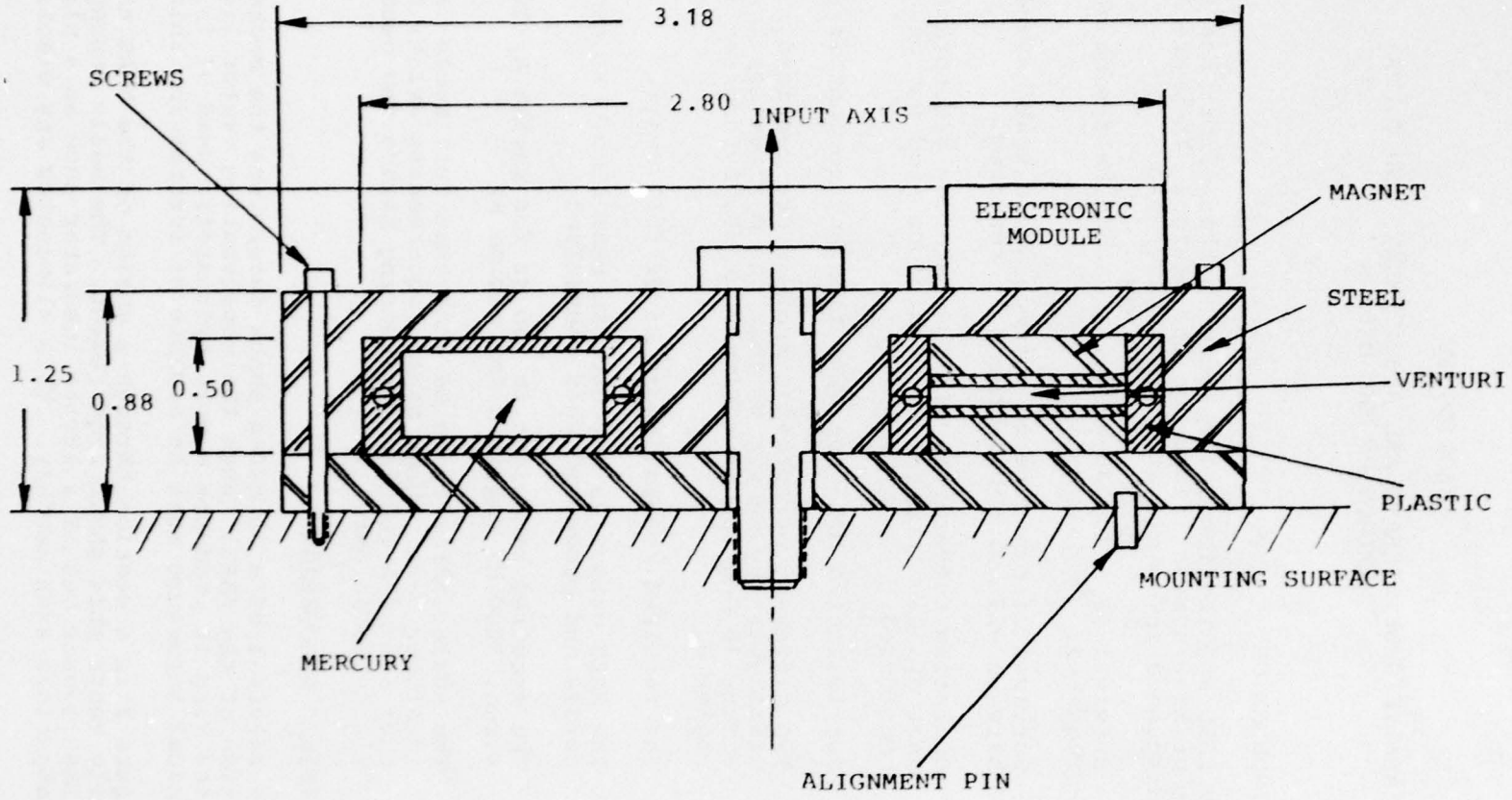

Figure 2. KARS Unit - Crossectional View

problems relating to shorting the mercury to case ground, and also eliminates contamination of the mercury. This plastic structure is not sufficiently strong to sustain the 15,000 psi; that is accomplished by potting the plastic into a strong steel container. This container has been analyzed on a worst-case basis, assuming a uniform 15,000 psi pressure within the mercury rather than a gradient. It survives this condition with maximum stresses at or below 80,000 psi. This range of strength is easily achieved in a variety of stainless steels without heat treatment; with heat treatment, double that strength can be achieved.

The following discussion gives the details of the analysis. The assumptions are:

1. The pressure is uniform throughout the mercury.

2. All structural loads are carried by the metal outer structure.

Due to symmetry, this structure could be modeled as a circular plate, with a circular hole, both edges supported and fixed with a uniform load (the internal pressure) over the entire surface as shown schematically below.

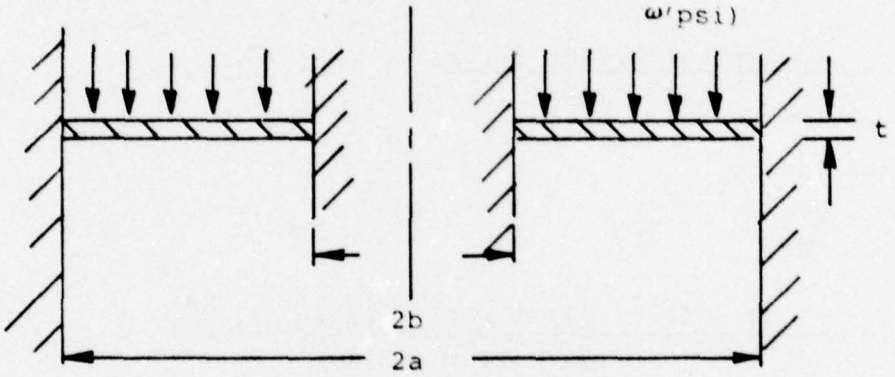

The limiting stress, shear and deflection can be calculated from formulas given in Roark Formulas for Stress and Strain, McGraw Hill (Case 77 Page 237) 4th edition.

Maximum stress occurs in radial direction $S_r = \frac{\omega a^2}{t^2}$

Maximum deflection $y = \frac{a^4}{ET^3}$

Edge shear per linear inch $V = K_{\omega}a$

for our case a/b = 1.78. The following coefficients are tabulated in Roark.

$\beta_{outer} = 0.0855$

$\beta_{inner} = 0.1097$

$K_{outer} = 0.1913$

$K_{inner} = 0.2545$

$\alpha = 0.00137$

$\omega = 12{,}700$ psi

Using an ultimate tensile stress of 100,000 psi, E = 30 X 10^6 psi and a safety factor of 1.5/1, the material thickness can be determined from the worst case condition (inner wall):

$$t = \sqrt{\beta\omega/s_p} \qquad (6)$$

$$= \frac{(0.1097)\ (12{,}700)\ (1.5)}{(1 \times 10^5)}\ (1.3) = 0.188 \text{ in.}$$

the deflection is

$$y = \frac{a\omega a^4}{Et^3}$$

$$y = \frac{(1.37 \times 10^{-3})\ (12.7 \times 10^3)\ (1.5)\ (1.3)^4}{(30 \times 10^6)\ (0.188)^3}$$

$$= 2.88 \times 10^{-4} \text{ in.}$$

The shear stress would be minimum at the outer edge.

$$\delta_s = \frac{K\omega a}{t}$$

$$= \frac{(0.1913)\ (12.7 \times 10^3)\ (1.5)\ (1.3)}{0.188}$$

$$= 25{,}200 \text{ psi}$$

The longitudinal and hoop stresses at the outside edges can be determined from thin-walled stress theory. With a 0.190 in. thick wall, the levels are 34,600 psi and 30,950 psi, respectively. The stresses calculated are based on conservative models and will be used as design criteria for the evaluation units. They result in a combined stress below 80,000 psi and are considered acceptable. A sketch of the crossection of the unit is shown in Figure 2 with typical dimensions.

The wide range of temperature soaks also produces a stress condition because mercury expands much faster than most solids.

The approach settled on is to use the "O Ring" seal which is required for sealing purposes as the compliant structure which prevents thermally-induced pressure buildups.

Volumetric calculations show that a radial deformation of the O-ring of 0.001 in. is sufficient to accomodate the expansion required by the thermally-induced bulk modulus effect on pressure. Based on manufacturers compatibility charts, a Nitrile rubber (Parker Seal Company compound N674-70 Buna N) has been selected.

A typical breakaway friction force level permitting the O-ring to deform would be 110 pounds. This is based on manufacturers supplied data, and a static face seal configuration. Pressure forces available at 2000 psi (basis for friction force calculation) would be 1230 pounds so there is ample force to overcome the friction and deform the O-ring. An additional benefit is derived through bulk compression of the O-ring under pressure. Extrusion of the O-ring is prevented by the line-to-line fit of mating surfaces in a static face seal.

A further advantage of the O-ring configuration is found in its capacity to absorb acoustic energy. Acoustic noise generated in the mercury will be attenuated by the compressibility of the O-ring.

The operating temperature is considered to be relatively constant for several reasons:

- The KARS is relatively massive in itself and it is usually anchored to relatively large masses which provide thermal inertia. Since the time of actual use is very short, a temperature change in that period is unlikely.

- The KARS is mounted in the test structure for a relatively long period of time before use, usually days. Therefore, it has achieved thermal equilibrium with its surroundings.

- The power dissipation within the sensor is nil. Therefore, operation doesn't produce temperature variations within it. On the other hand, the electronics consumption is expected to be in the order of 2 watts. This is considered small enough to be ignored since they are outside the sensor package.

As a result of this favorable thermal configuration heaters and temperature controllers are considered unnecessary in the design. Also special insulation is also considered unnecessary.

The vibration requirement is of the transportation survival type. The operating environment doesn't produce a sinusoidal input to the sensor. By its nature it contains shocks rather than a ringing type motion. As a result no special vibration isolation is required. On the other hand, vibration tests on a model of the KARS show no output for linear vibrations of 5 g's in. below 1100 Hz.

The scaling, bandwidth resolution and processing of the KARS output in this specific application are not easily separated. They involve the electronics design and some mechanical considerations, and the fact that the data is not used in real time. The following discussion explains the approaches taken.

There are two distinct sets of input conditions which the KARS is expected to experience. They come about because it is desired to instrument two distinctly different phenomena. The inputs are tabulated below.

Table 1. Input Regimes

PARAMETER	REGIME 1 (COND A)	REGIME 2 (COND B)
Maximum input rate,°/s	10	30,000
Bandwidth,Hz	500	5,000

In the interest of minimizing the inventory of sensors required and reducing the possibility of improper selection, it is desirable for one sensor to be capable of instrumenting both input regimes. This does not pose a formidable problem. Unlike rate gyros where maximum rate capability is inherent in the mechanical design, the KARS has no mechanical restriction on maximum rate. Therefore, the problem in performing in two regimes is electronic in nature.

The problem is twofold. Scaling must be adjustable to give 5 volts out for either 10°/s or 30,000°/s. A low-pass filter corner of 500 Hz is required for the former, and 5000 Hz for the latter. The first thought was to provide adjustments in the form of external buses that connected the correct gain set and frequency corner variations. Upon reflection, however, this is not the best approach. It is needlessly complex and, in use, has inherent possibilities for errors. It is almost certain that, eventually, some improper permutation of the bus connections would be used.

The simpler scheme is presented here. It takes advantage of the fact that the KARS output is not used in real time; therefore, the filter corner can be set at 5000 Hz. Any data produced in Regime 1 can be reprocessed through a 500-Hz filter at the users convenience. This reduces the problem to providing the correct gain to output 5 volts for either a 10°/s or 30,000°/s input. This is accomplished by staging the gain on the correct multiples. In this case, assuming the output at the terminals of the sensor package is 4 μV/°/s, the gains are readily calculated. In order to output 5 volts for an input of 30,000 °/s, a gain of 41.6 is required. In order to output 5 volts with an input of 10°/s, an additional gain factor of 3000 is required. Therefore, an amplifier package with a gain of 40 followed by a unity gain 5000 Hz low-pass filter, and this followed by a gain of 3000 can satisfy the gain and bandwidth requirements of both regimes.

In summary, the KARS connector will have 2 outputs. One will be low gain, 40, and a low pass corner of 5000 Hz. The other will be high gain, 120,000, and a low pass corner of 5000 Hz. The user has the option of recording either or both signals and can also, if desired, reduce the bandwidth by further processing after the fact. Figure 3 represents the system schematically.

The resolution of the KARS is a function of noise on its signal and the intrinsic gain of the sensor. In order to achieve the design goal of 2.0% of full scale, it was necessary to take specific steps to reduce the noise and enhance the intrinsic gain.

5.1 Resolution/Noise

Analysis of the KARS revealed only two significant noise sources. They were the voltage noise in front end of the input amplifier and the Johnson noise in the current flowing in the mercury ring. The latter was in the order of 10^{-10} volts and could be disregarded. The former, however, is large in most amplifiers and a survey of available amplifiers was undertaken. The result was selection of the PMI SSS 725 Instrumentation Amplifier.

The noise voltage for the PMI725 Instrumentation Amplifier is determined from the equation:

$$N = 6.8 \left[6.5 \ln f_2/f_1 + f_2 - f_1\right]^{1/2}$$

N = RMS Voltage Noise in nanovolts

f_1 = Low frequency corner

f_2 = High frequency corner

For the design goal of f_1 - 5000 Hz, f_2 = 0.01 Hz, we get N = 0.48 microvolts. For the design goal of f_1 = 500 Hz, f_2 = 0.01 Hz, we get N = 0.016 microvolts. Both clearly dominate the sensor package noise and therefore, define the threshold of the instrument.

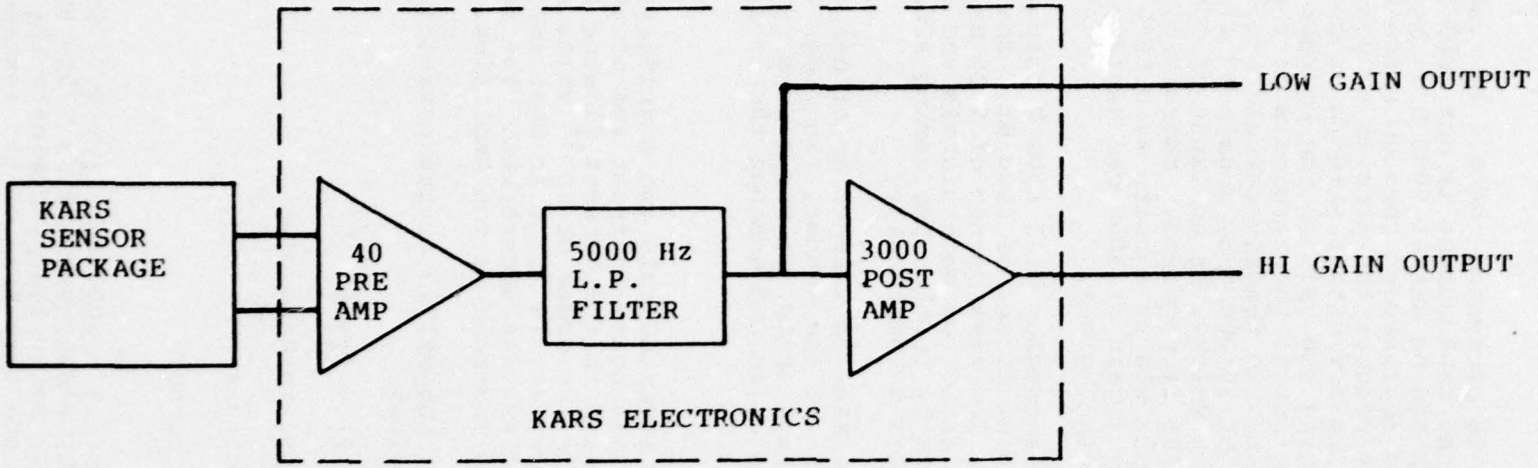

Figure 3. KARS Block Diagram

Using a scale factor (at the terminals of the sensor package) of 4 μV/°/s, the threshold is 0.12°/s for the first case and 0.004°/s for the latter.

Since full scale for the worst case is 10°/sec and assuming that the minimum detectable signal is the RMS noise level we get the threshold of 0.12°/s/10°/sec or 1.2% which satisfies the design goals.

Special efforts were needed to achieve the design scale factor (at the terminals of the sensor package) of 4 microvolts/deg/sec. These were based on an analysis of the basic pickoff equation. The KARS pickoff consists of two electrodes submerged in the mercury separated by a distance, L. A magnetic field of flux density, B, is oriented perpendicular to the tangent of the mercurys path. When the case moves with a velocity, V, relative to the mercury, a voltage E appears across the electrode according to the following law:

$$E = BLV$$

Two options are available, increase B and increase V. Both were exercised.

The original KARS pickoff employed two samarium cobalt magnets. They were in the readily available form of 3/4-X 3/4-X 3/16-in rectangular prisms. Operating over the normal range of clearances found in the KARS design they produce flux densities in the kilogauss range. Figure 4 is a flux density vs gap curve for these magnets.

Two design refinements are used to optimize flux density. First, a return path of soft iron is planned. This will complete the magnetic circuit between the two magnets, enhancing the flux density in the gap and reducing stray flux near the instrument. The other change is to shape the magnets to concentrate the flux in the vicinity of the electrodes.

Figure 5 illustrates the concept of the shaped magnets. It is a schematic view of the venturi throat and magnets of a typical KARS. The magnet spacing is typically 1/2 inch which results in a flux density of 2,500 gauss.

It demonstrates advantages of the shaped magnet. The flux density in the gap and, therefore, the scale factor is increased for two reasons. First the shaped pole face tends to concentrate all the flux passing through the magnet over a smaller area. Second, because the width of the magnet is reduced, it becomes possible to partially bury it in the venturi throat. This reduces the reluctance of the gap.

The venturi throats locally increase the velocity of the mercury in the vicinity of the pickoff. Several models were built with various throat ratios. Up to a point there exists a clear relationship between throat ratio and scale factor. (This is discussed in detail in part 5 of this report.) At this point, it is sufficient to say that the combination of venturi throats and improved magnet design make the achievement of a scale factor of four microvolts/deg/sec a certainty at the terminals of the KARS sensor.

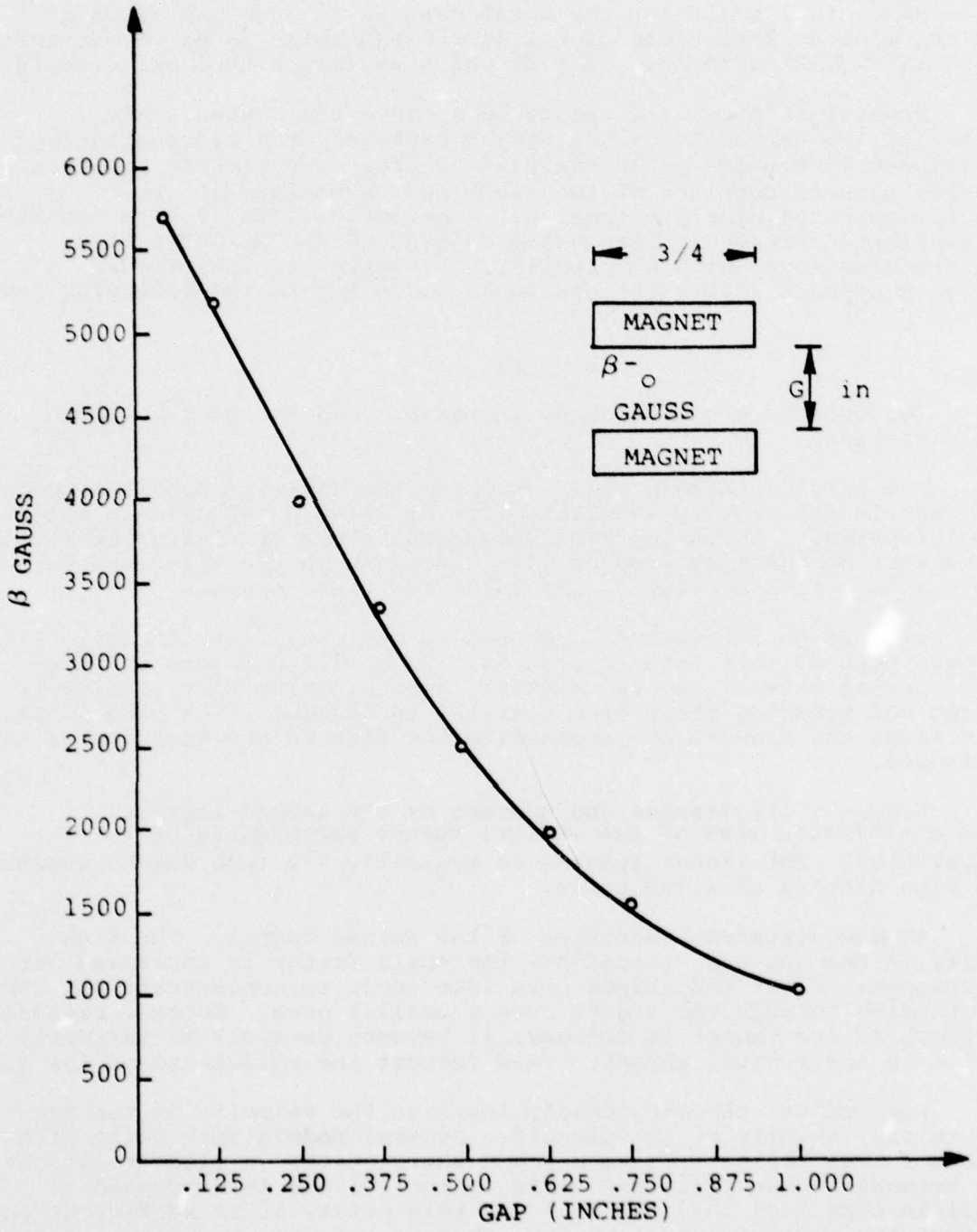

Figure 4. Flux Density Vs Gap

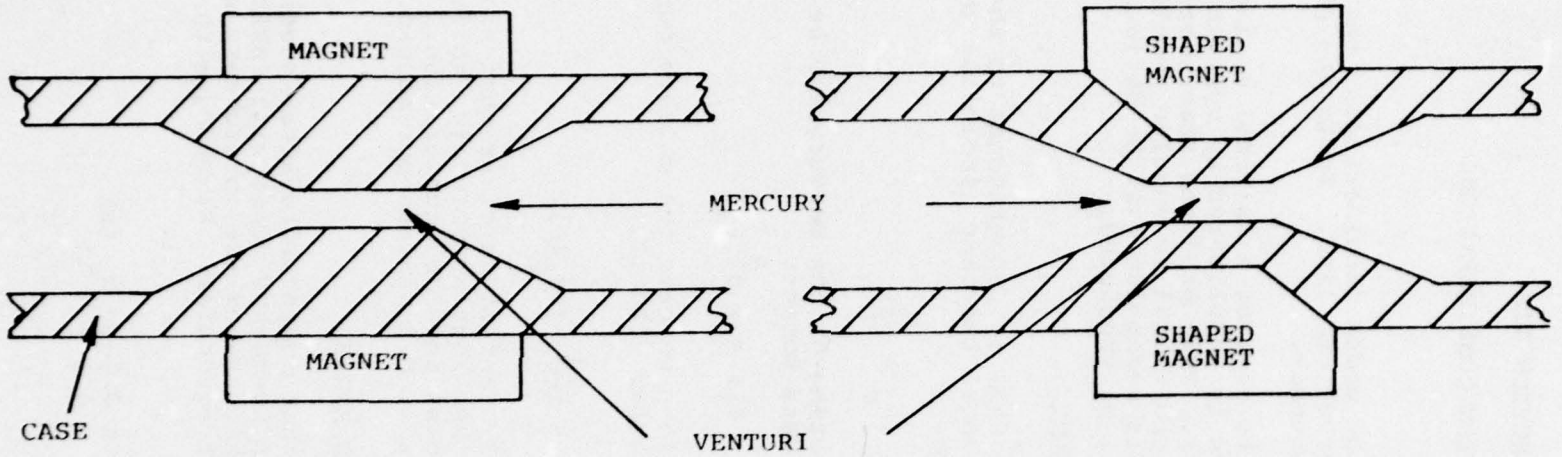

PRESENT PICKOFF CROSS SECTION
FIGURE 5a

IMPROVED PICKOFF CROSS SECTION
FIGURE 5b

Figure 5. Magnet and Pickoff Design

SECTION III

DATA REDUCTION CONSIDERATIONS

6. INTRODUCTION

In the specific mission under consideration, the analysis of the KARS output can be performed off line. Speed and phase shifts in real time are of no consequence.

It is important only to recover a faithful analog of the input angular rate. This objective is complicated by certain peculiarities in the KARS transfer function. This produces some contamination of the rate data with signal proportional to angular acceleration. In the following discussion, this mechanism will be defined and a rather simple correction scheme will be presented.

7. SENSOR OUTPUT CHARACTERISTICS

Voltage output of the KARS is proportional to the difference between the angular velocities of the case (including the probes and magnets) and the mercury ring.

$$e_o = K\ s\ (\theta_c - \theta_\ell)$$

The viscuous torque acting on the mercury can be equated to angular acceleration by its mass moment:

$$D\ S\ (\theta_c - \theta_\ell) = J\ S^2\ \theta_m$$

Combining these equations we have the voltage output expressed as a function of the case angular velocity:

$$e_o\ (s) = K\ \frac{\tau s}{1+\tau s}\ [s\theta_c(s)]$$

Here, τ is the ratio J/D and it is clear that high frequency response is proportional to case angular velocity, while low frequency response is proportional to case angular acceleration. The KARS has a corner frequency of 0.05 Hz or 0.3 radians per second.

8. UNCOMPENSATED ACCELERATION ERROR

Unprocessed raw data that are recorded after passing through a low pass filter to limit high frequency noise will exhibit a net acceleration error, so-called because of the instruments sensitivity to acceleration at very low frequencies. Starting with the output

$$e_o\ (s) = K\ \frac{s}{s + \frac{1}{\tau}}\ \omega_c\ (s) \qquad (a)$$

expressed in Laplace notation, it is necessary to model an input signal that characterizes the main features of the angular velocity:

$$\omega_c\ (t) = We^{-2t}\ (1 - e^{-250}t) \qquad (b)$$

Peak value of $\omega_c(t)$ occurs when t = 0.026 seconds and has the value 0.62 W. The maximum level of angular rate is specified as 10°/sec and here it has a rise time of 0.004 seconds with an estimated decay constant of one-half second. Taking the transform of ω_c (t) we have

$$\omega_c\ (s) = W\left[\frac{1}{s+2} - \frac{1}{s+252}\right]$$

If ω_c (s) is substituted into equation A the instrument output e_o (s) can be inverted to yield e_o (t). But we are concerned here with the error rather than e_o (t) itself and express that error in Laplace notation,

$$\varepsilon(s) = K\left[\frac{s}{s + \frac{1}{\tau}}\ \omega_c\ (s) - \omega_c\ (s)\right]$$

$$= K\left[\frac{1}{(s+\frac{1}{\tau})\ (s+2)} - \frac{1}{(s+\frac{1}{\tau})\ (s+252)}\right](-\frac{1}{\tau})\ W$$

Now take the inverse Laplace transform (with $\frac{1}{\tau}$ = 0.3 rad/sec)

$$E(t) = K\left[\frac{e^{-0.3t}}{1.7} - \frac{e^{-2t}}{1.7} - \frac{e^{-0.3t}}{251.7} + \frac{e^{-252t}}{251.7}\right](-0.3)\,W$$

$$= K\left[-0.175\ e^{-0.3t} + 0.176\ e^{-2t} - 0.001\ e^{-252t}\right] W \qquad (c)$$

The last term in brackets must be less than 0.02 to meet the instrument specification of less than 2 percent error. Computation shows a maximum rate error in excess of 40 percent in the following error table of transient angular rate. Maximum range is proportional to W so that percent error is unaffected by sensor range.

Rate Error vs Time

t		Error ÷ W	
0	seconds	0	degrees per sec/max°/sec
0.1	seconds	0.13	degrees per sec/max°/sec
0.25	seconds	0.306	degrees per sec/max°/sec
0.5	seconds	0.403	degrees per sec/max°/sec
1.0	seconds	0.266	degrees per sec/max°/sec
1.5	seconds	0.13	degrees per sec/max°/sec
2.0	seconds	0.0580	degrees per sec/max°/sec
5.0	seconds	0.0002	degrees per sec/max°/sec

Clearly, the data must be processed. The sensor characteristic is compensated readily by proportional plus integral means that are essentially exact using the function F acting on the sensor transform:

$$\frac{s}{s + \frac{1}{\tau}} \cdot F \approx 1$$

so that

$$f = 1 + \frac{1}{\tau s}$$

It can be shown that uncompensated angular rate measurement errors reach and exceed 2 percent at frequencies of 18 Hz and below.

9. DATA PROCESSING

Low noise at the input to the operational amplifier obviates the need for a sophisticated filter to optimize data recovery. This means, also, that recording of the raw data is a viable procedure followed by off-line processing. Whether or not the KARS output is band-limited, it would be both prudent and simple to insert band-pass filters in front of the recording equipment with cut-offs at about 5 kHz for the high bandwidth application and 500 Hz for the low bandwidth application. Subsequent processing will be necessary since there is a significant error due to acceleration in the frequency range below the instrument corner frequency of 0.05 Hz. It was shown that mixing the direct signal with its integral can yield an exact representation of angular rate at low frequencies so that the only error concerns the accuracy of the model $\frac{s}{s+1/\tau}$ and the matching filter $1 + \frac{1}{\tau s}$.

SECTION IV

DEFINITION OF TEST REQUIREMENTS

10. INTRODUCTION

A satisfactory test program is one that demonstrates that a device can perform its mission satisfactorily and calibrates the device so that its output can be properly interpreted. Type tests need be performed only on selected units demonstrating that certain design criteria have been satisfied. Other tests must be performed on every instrument either for calibration purposes or because inadequacy would produce a catastrophic failure.

The discussion of the test plan will start with type tests. The assignment of a test to this category is based on engineering judgement and the desire to avoid repeating tests which are not expected to yield significant results. On the other hand, should type testing reveal unexpected problems or results inconsistent with existing understanding that test would be performed on every unit.

The test plan is summarized in Figure 6.

11. TYPE TESTS

In the case of the KARS, type testing on selected units is recommended for the following parameters:

1. Low Frequency Corner - This is the frequency associated with $1/\tau$ in Equation (6) in section 3. This parameter is a function of the inertia of the mercury, it is associated viscous drag, eddy current drag produced by the magnets and drag effects produced by the venturi sections. It is unlikely that any of these parameters could change enough as a result of tolerances to have a significant effect on τ. Also it is unlikely that a catostrophic failure could occur without being obvious during calibration. Therefore, type testing is indicated for this parameter.

   The specific test is straightforward. The KARS output signal issued to form a Lissajous pattern with the tachometer output of the rate table. Then the frequency is varied until a 45-degree phase shift is detected defining the low corner frequency.

2. Electronics Sensitivity to Supply Voltage - This characteristic of the amplifier design is easily controlled. It is not likely to be unsatisfactory in a working amplifier. Consequently, it is suitable for type testing. The test itself is to measure the instrument scale factor

Acceptance Tests	Type Tests
Scale Factor	Low Frequency Corner Evaluation
Electronics Gain Settings	Electronics Sensitivity to Supply Voltage
Resolution	Sensor Weight
Electronics Bandwidth	Temperature Soak Survival
Vibration Survival	Temperature Soak Operation
Maximum Input Rate	Thermal Shock
Mechanical Shock	Magnetic Sensitivity

Figure 6. Recommended KARS Test Plan

at a convenient frequency (near 20 Hz) with the amplifier supply voltage at the high and low extremes. These values of scale factor are compared with the calibrated scale factor.

3. Weight - The sensor weight is not a critical parameter; nor is it likely to vary significantly from unit to unit. Consequently, this parameter is type tested. The weighing means is a conventional platform balance.

4. Temperature Survival and Operating and Thermal Shock - The temperature survival test verifies the design concept associated with the compliance of the O-ring as discussed in Section 2. Once the design is established and verified, failures not detected in shock, vibration and routine handling are unlikely. This is also true of thermal operating tests which require a slightly smaller temperature excursion. The thermal shock tests involve relatively slow changes in the mechanical properties of the sensor as a result of its relatively large heat capacity. Therefore, this test will also be considered as a type test.

   All thermal tests will take place in standard environmental chambers. The operating test will involve measurements of the noise level and bias level at the extreme temperatures and other temperatures as needed. Measurement of scale factor at temperature extremes is extremely involved because conventional laboratory test equipment will not function. Development of effective test equipment is not practical, although it is possible.

5. Magnetic Sensitivity - The magnetic flux density in the KARS pickoff is quite high, over 1000 gauss. The scale factor is linearly proportional to this parameter; therefore, variations in the local magnetic field consistent with terrestrial variations are unlikely to have any effect. Consequently, magnetic sensitivity is a reasonable choice for type testing. The specific test will be a measurement of the KARS scale factor on a rate table in the presence of a set of Helmholtz coils.

12. ACCEPTANCE TESTS

The following tests are recommended to be performed on every deliverable unit.

1. Scale Factor, Gain, Resolution - These three parameters are measured while operating the KARS on a precision rate table. The instrument should be calibrated at a standard frequency in the order of 20 Hz. It should also be checked at the maximum frequency available on the table and a frequency in the order of 1 Hz. The two gain settings

are evaluated as part of this measurement. If the noise level is also measured at this time the resolution can be calculated.

2. Bandwidth - This is a purely electrical parameter. It is evaluated during the electronics checkout.

3. Vibration Survival - This is a good test to verify the ability of the KARS to withstand normal handling. It also weeds out a variety of potential problems including loose screws, poor solder joints, etc. The specific test is MIL Standard 810-C, Method 514, Figure 514.2-7 Curve AV for a 12-minute logarithmic cycle.

4. Maximum Input Rate - No good test is available for 30,000 deg/sec. This value is 2 orders of magnitude higher than can be achieved on Kearfott rate tables. However, when considering the operating principle of KARS it becomes apparent that performance is best for high rates and frequencies. Under these conditions the mercury behaves as a rigid body. No viscous effect influences its velocity profile. Therefore, the output should be directly proportional to rate.

   The only test that is possible requires the associated test equipment to be built. In this approach, the rate sensor will be mounted on a shaft which in turn is mounted on bearings. A potentiometer is mounted on the shaft. The shaft is rotated vigorously through a small angle into a stop. Then the output of the KARS is compared with the differentiated output of the potentiometer. It is estimated that rates in the order of 1000 deg/sec can be achieved. The difficulty is that the differentiated potentiometer output may be too noisy to permit comparison to within 2%. However, this approach should expose any gross defects.

5. Mechanical Shock - The mechanical shock requirement of 10,000 g is the most important non-performance design requirement imposed on the KARS design. It also seems to be the most likely source of failure. Therefore an effort should be made to test every unit as near as possible to that requirement.

   The best available commercial test equipment that will achieve shocks in this range cannot sustain the levels anywhere near the time duration required. A typical machine manufactured by the Avco Corp. with a special shock amplifier adapter kit, can generate a 10,000-g saw tooth pulse but with a pulse duration of only 0.10 milliseconds. This time duration is 1/30 of the requirement, but could serve as a convenient go/no-go test.

SECTION V

CRITICAL SUBASSEMBLY TESTS

13. INTRODUCTION

The purpose of this portion of the effort was to generate data that aid in designing a production model of the KARS and to show that the performance and environmental requirements could be met. Six tests were specified:

Thermal Storage Survival

Shock Survival

Performance In Vibration

Performance During Shock

Calibrated Input (Scale Factor)

Evaluation of a Push Pull Electrode Configuration

Many other tests were also performed.

14. DISCUSSION OF SPECIFIED TESTS

14.1 Thermal Storage Survival - This test was intended to be performed on a subassembly that would demonstrate the ability of a porous metal foil to act as a very stiff bellows when submerged in mercury. The basic principle is that the surface tension of mercury which is very high prevents it from being pushed into the capillaries in the porous metal.

The pressure, P, required to push mercury into a hole of radius, γ, against its surface tension θ acting at a contact angle ϕ is

$$P\ (\pi\ \gamma^2) = 2\pi\ \gamma\ \sigma\ \cos\ \phi$$

$$\text{or } P = \frac{2\sigma\ \cos\phi}{\gamma}$$

For holes of the order of 1 micron in diameter the pressure ΔP is in the order of 150 psi. Porous metals are commercially available with pore sizes in the micron range. The total void volume of such materials is 30%.

Assuming: 0.94 cubic inches of mercury, a differential expansion of 150 ppm/c° and a maximum temperature swing of 55°C we get a change in volume of 7.7×10^{-3} inch^3. This is equivalent to the void volume in 25×10^{-3} inch^3 of the porous material.

An experiment was run to verify the validity of this approach. A 416 stainless steel container with a volume of 0.94 inch cubed was filled with mercury and sealed. It was instrumented with a pressure transducer, then it was heated. Pressure vs. temperature was recorded.

The test was repeated with a significant volume of porous metal included. No change in the pressure vs. temperature curve was noted. The problem appears to have been that the void volume in the porous metal was much smaller than the design value. In other words, we were unable to drive the mercury into the voids that did not lie on the immediate surface.

These tests did lead to the approach currently being used. It was noted that the pressure rise in the container was much smaller than predicted with or without the porous metal. This was traced to the compliance of the "O-Ring" seal.

14.2 Shock Tests - 10,000-g shocks are not achievable in commercially available test equipment with time duration required. The only way to achieve that level is in an airgun or cannon.

Singer Kearfott has in its environmental test lab an AVCO Model SM-005-3 Shock Test Machine. The maximum capability of this machine is 2200 g's with a 0.25 millisec duration.

One of five venturi configurations (a 4/1 model, the ratio of which refers to the increase in local velocity, V, by an area reduction at pickoff electrode plane) was potted with its electronics in an aluminum shell with General Electric RTV 634. A reference scale factor measurement was made and the unit subjected to the shock testing. A series of five shocks were inputted starting at 600 g's (0.7 millisec duration) and ending at 2200 g's (0.2 millisec duration). No visible damage was observed and when the scale factor was checked no change was observed or shift in the bias level.

The last 2200 g shock test was repeated for a total of six shock tests and during this test the output from the KARS was monitored. Figure 7 shows two photos of the traces recorded on a fast writing memo scope. Figure 7a shows the pulse shape of the shock input while Figure 7b shows two traces, the upper being the output from the KARS and the lower being the pulse shape at an uncalibrated scale setting and only used as a time reference. As the trace indicates an input was sensed by the KARS and an output generated. This output is felt at this time to be due to the drop test table motion as impact which is common with this type of machine. A more sophisticated test with an optical displacement sensor would have to be performed if this turns out to be a problem.

14.3 Temperature Tests - The 4/1 potted unit was subjected to a limited thermal cycle. The reason for the limit is that this unit does not contain any thermal compensation mechanism to allow operation over the entire thermal range. A temperature cycle of 80°F to 50°F to 0°F to 80°F was used with a 20 min. soak at each

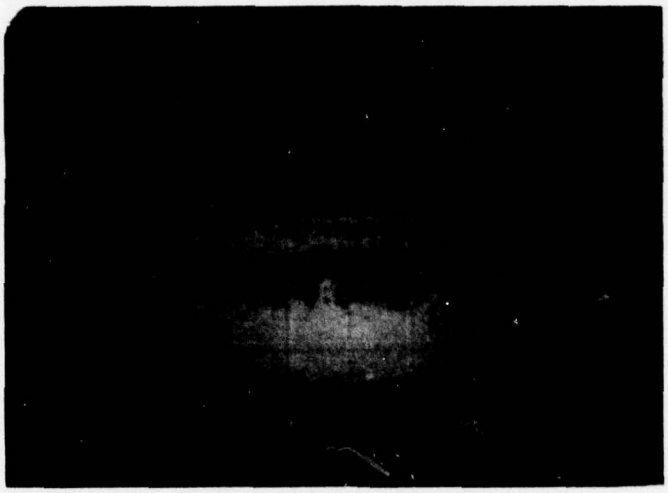

2200 g's 0.2 millisec duration

a. Shock Input

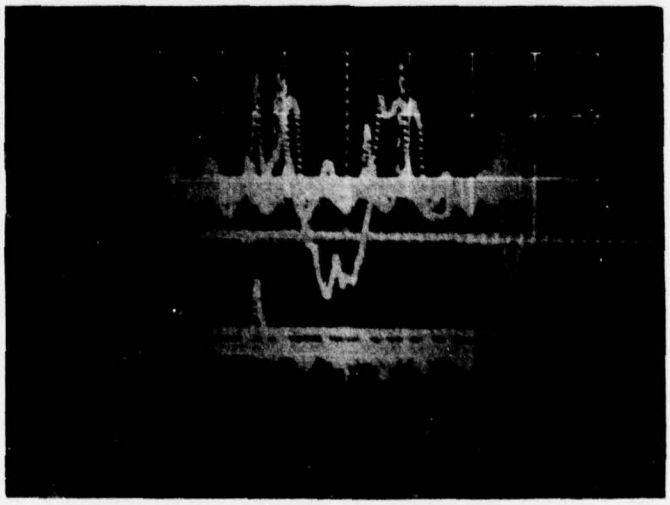

2200 g's 0.2 millisec duration

b. Top Trace - Instrument Response
Bottom Trace - Shock Input

Figure 7. Shock Test

temperature. The D.C. bias voltage was monitored during the testing and a maximum deviation of -10 millivolts was observed at 0°F. This cycle was repeated twice. The unit was then heated in 10°F steps to 100°F with a similar soak time and deviation in the bias level was observed. Under all conditions the initial zero bias level repeated. After the thermal soak tests were completed the units scale factor was checked to the initial reference value and good agreement was obtained.

14.4 Vibration Tests - The 4/1 potted KARS unit was subjected to the MIL Std 810B transporation spec Figure 514-6 Curve AB and survived. Scale factor testing pre and post testing showed good agreement. To obtain some insight into the behavior at higher frequencies, sine sweeps starting at 1g and going up to 5 g's at 20-2000 Hz were made. During the final 5g run the KARS output was monitored and showed a resonance peak at 1400/1500 Hz equivalent to 13.5°/sec showed no effect of the resonance on performance. As survivability was of major importance no work was done to identify the source or eliminate by isolation the resonance observed.

In conclusion all of the scale factor data was plotted on one curve and appears as Figure 8 in this section. As the plot shows the scale factor is 2.23 MV/°/sec and no apprecialbe change due to the environmental tests previously discussed.

14.5 Calibrated Input - Scale factor testing was performed using a Genisco Model 1300-5 Rate Table with an auxiliary input option. With this option variable dynamic rates at various frequencies could be used as control inputs to the KARS. The rate table is equiped with a tach generator so that actual input rates and frequencies can be measured. Table 2 shows a typical test log indicating the rates and frequencies used as a basis for determining the KARS scale factor. The maximum rate at the given frequencies represent the linear response limit set by the manufacturer.

Five different venturi configurations were designed, built and tested. These are referred to as 1/1, 2/1, 4/1, 8/1 and 16/1 models. (The ratio refers to the increase in local velocity, V by an area reduction, at pickoff electrode plane.) Figure 9 is a plot of scale factor vs. velocity ratio which represents a summary of all the data recorded. As expected the scale factor increased with an increase in velocity, V. The low frequency corner response was also evaluated by utilizing the tach output and the sensor output in a Lissajous pattern and these data are summarized in Figure 10. The specification requirement of 1 Hz for this corner determines the maximum velocity and then from Figure 6 the associated scale factor for this configuration. Under these conditions the optimum velocity ratio would be 12/1 and the scale factor would be 2.83 MV/deg/sec. (based solely on velocity improvement). This scale factor represents a 9/1 improvement in the original engineering model.

Table 2. Typical Test Log

C=330 pf
R=887 K-ohms
F_c=540 Hz

f=10 Hz
pp

	Rate °/sec	Tach rms	Sensor Output cm mv/cm	pp Output mv	OP Output mv	Scale Factor mv/°/sec
	5	.247	1.4 × 5	7	3.5	.70
	10	.495	2.9 × 5	14.7	7.4	.74
	20	.990	2.8 × 10	28	14	.70
	30	1.485	2.1 × 20	42	21	.70
	35	1.732	2.5 × 20	50	25	.71 / .71
SCALE FACTOR			~~20~~			
	2	.099	1.6 × 2	3.2	1.6	.8
	4	.198	3.0 × 2	6.0	3.0	.75
	6	.297	1.8 × 5	9	4.5	.75
	8	.356	2.2 × 5	11	5.5	.69
	10	.495	3.1 × 5	15.5	7.8	.78
	12	.593	3.85	19	9.5	.79
	14	.693	2.1 × 10	21	10.5	.75 / .76

$\phi = \sin^{-1} A/B$

AVG = .74 MV/°/sec

	f	A	B	A/B	φ
FREQUENCY RESPONSE	10	0	4.3	0	0
	1	~~.05~~	3.7	0	0
	.1	.8	3.6	.222	12.8
	.05	1.62	3.2	.375	22.0

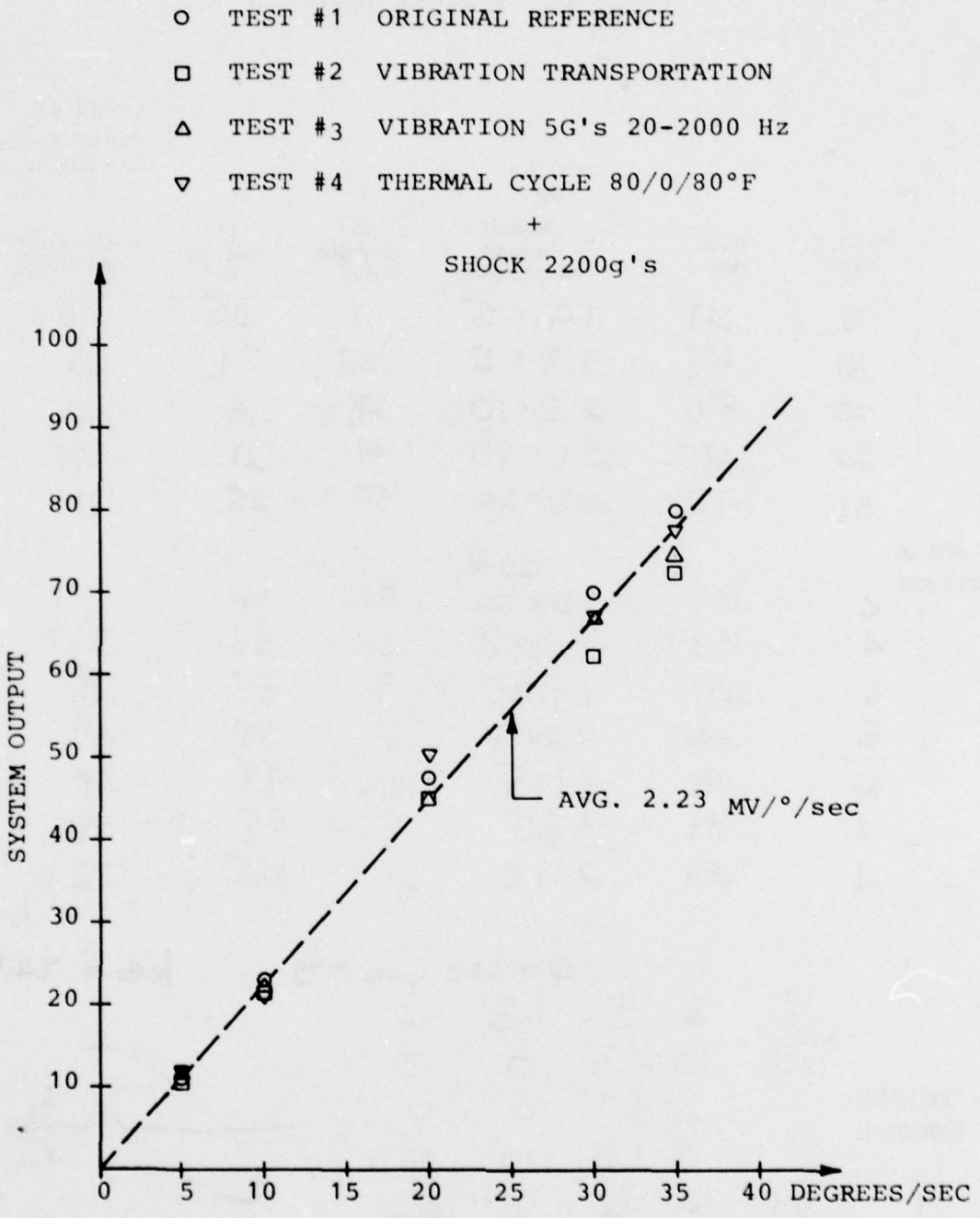

Figure 8. Environmental Effects - KARS Output Vs Input Rate 10 Hz After Various Exposures

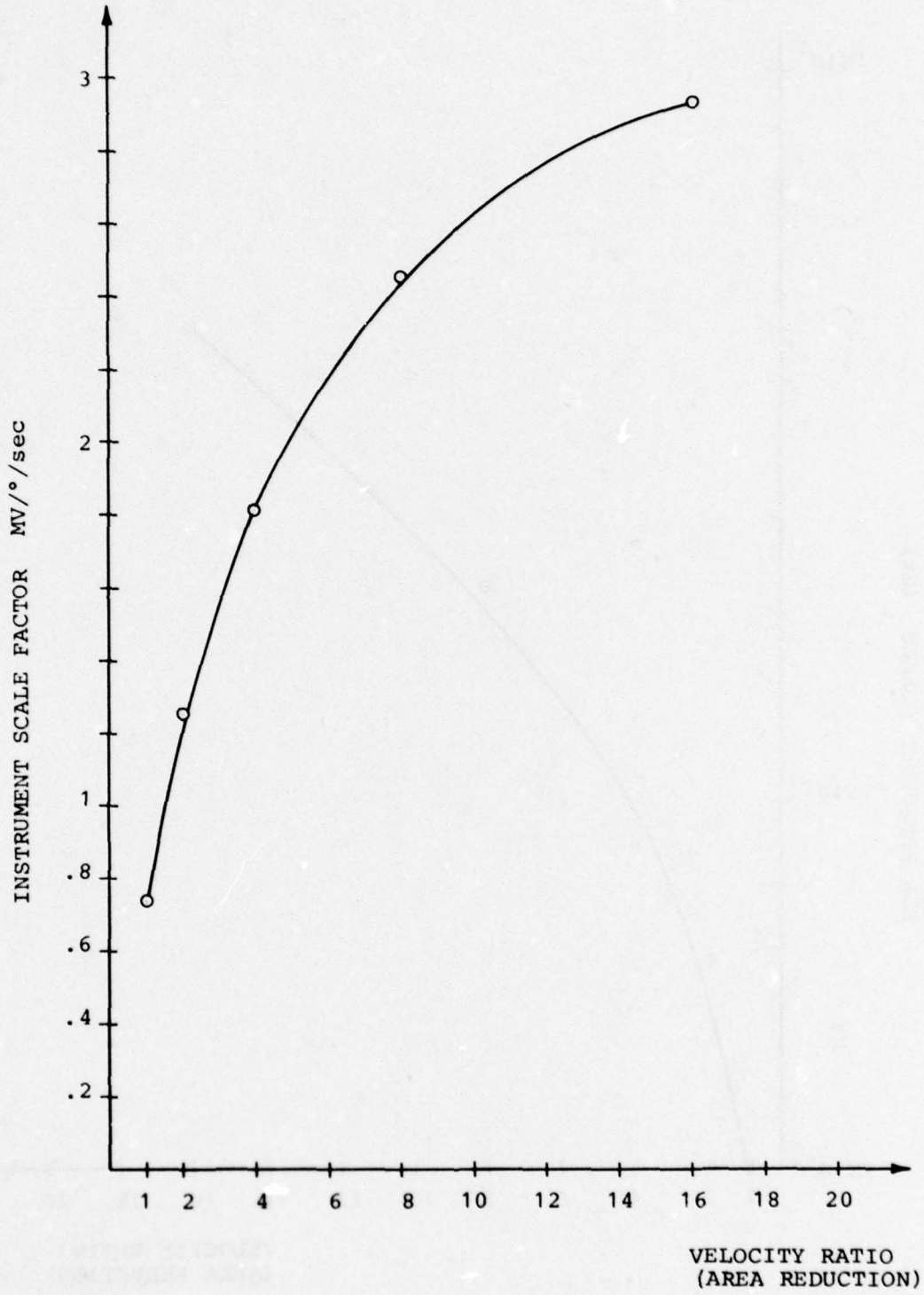

Figure 9. KARS - Instrument Scale Factor vs Velocity Ratio

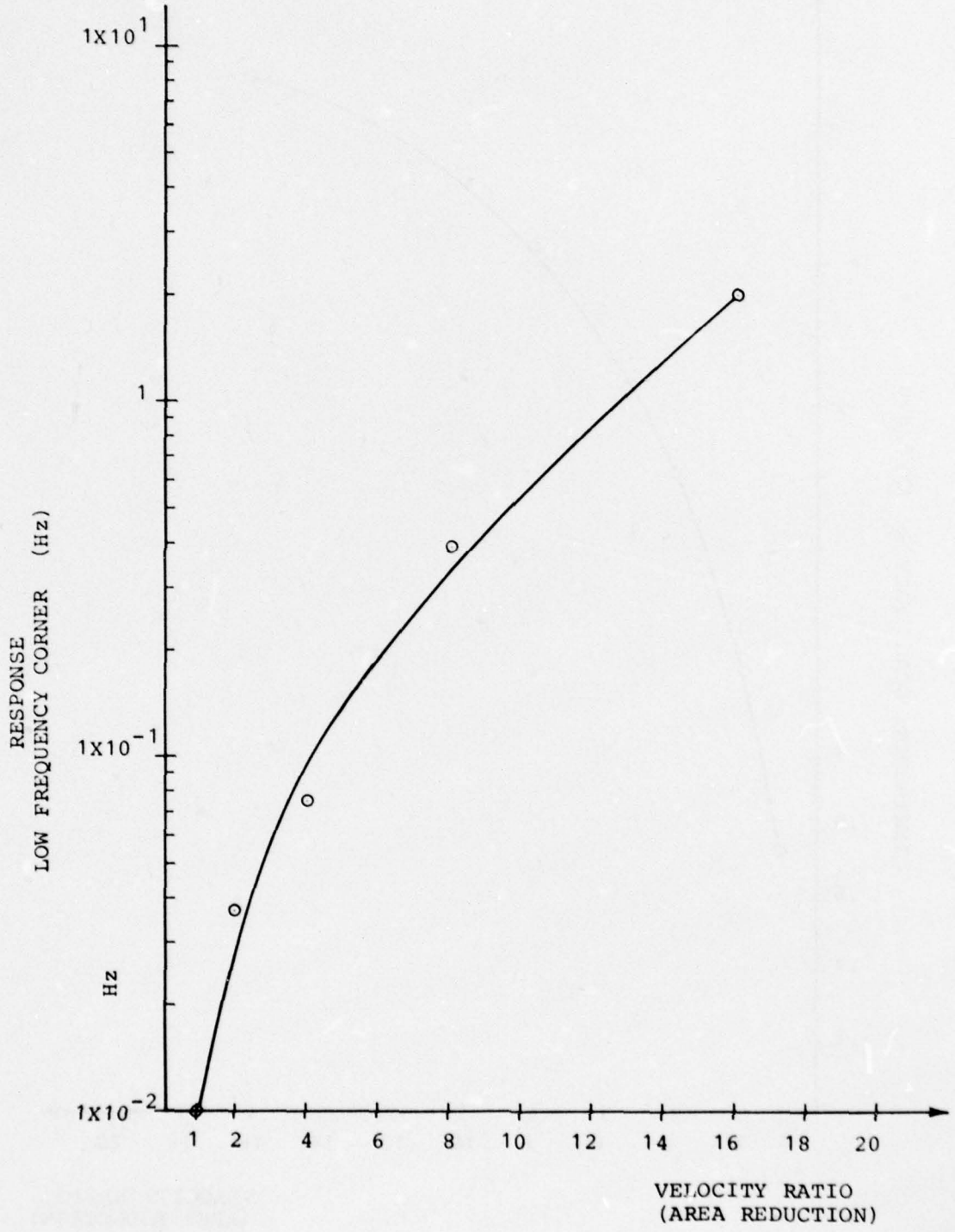

Figure 10. KARS - Low Frequency Corner Response vs Velocity Ratio

Additional scale factor information has been obtained using the 8/1 model on the Micro g Rate Table in the Kearfott Environmental Laboratory. The instrument was evaluated over a range of input rates from 0 to 30°/sec with a frequency variation of 10 to 100 Hz, and repeated the established scale factor of 2.5 MV/°/sec. At this time there does not seem to be observable limit or change in the instrument response at higher frequencies or rates.

14.6 Multiple Pickoff Mode - In the interest of increasing the scale factor a multiple pickoff scheme was considered. A dual pickoff version was designed and tested . Various connection configurations were tried,but the one that functioned best involved connecting the two outputs in a voltage adding circuit using one PMI SS725. Under these conditions, a two to one increase in scale factor was obtained. There was not significant change in the lower corner frequency response, or in the noise level of the unit. With respect to the noise this is explainable as the main source of noise is generated by the input stages of the processing amplifier rather than the pickoffs. Concerning the frequency response the drag induced by incorporating a second pickoff is small so there should be no effect. Based on this significant improvement a four pickoff 1/1 model was designed built and tested. As expected a four to one increase in scale factor over a single pickoff mode was measured. The ultimate extension of this improvement would be to have a large finite number of pickoffs located in a common magnetic field. This improvement in scale factor can simply be obtained by providing the pickoff electrodes and adding one additional resistor per pickoff to the electronic amplifier adding circuit.

Equivalent scale factor increase can be obtained by modifying the electronic gain by the same ratio which certainly is easier to do. To determine the advantage of one method over the other noise measurements were made of the two approaches. The data obtained are summarized in the following Table.

Table 3. Additional Pickoff Mode

NUMBER OF PICKOFFS	SCALE FACTOR (MV/°/SEC)	NOISE * (MV)	(°/SEC)	GAIN	ELECTRONIC GAIN MODE SCALE FACTOR (MV/°/SEC)	NOISE (MV)	(°/SEC)
1	1.83	0.8	0.44	1	1.83	0.8	0.44
2	3.86	1	0.26	2	3.57	1	0.28
3	5.57	1	0.18	3	5.57	2	0.36
4	7.10	0.8	0.11	4	7.14	3	0.42

*OP Measurements

The additional pickoff mode has, in each case, the same scale factor as the electronic gain mode. However, the additional pickoff mode has a significant advantage in signal to noise ratio; therefore, the resolution in the additional pickoff mode is improved.

No appreciable change in the noise was obtained by dropping the absolute value of the amplifier gain resistors, but maintaining the same gain.

All of the noise studies were made with a 500 Hz corner frequency filter in the line (Condition A Requirements).

14.7 Related Subassembly Tests - Basic magnetic flux measurements were made versus gap for various size Samarium Cobalt magnets and are included as Figures 11 and 12. These curves were used to judge the improvement in scale factor by increasing the magnetic flux when the gap is reduced. All of these measurements were made with a Radio Frequency Laboraties Model 1890 gauss meter in air with no return path. By incorporating a return path, testing at a particular gap (0.33 in.), a 45% to 5000 gauss flux density was measured.

Incorporating shaped pole pieces (4/1 area reduction) did not effect drastically the end conditions of a flux density versus gap, but did effect the shape of the curve as can be seen from comparing Figures 11 and 13. These measurements were made on off the shelf rectangular magnets that were used on all the KARS discussed in this report.

A special shaped configuration was fabricated, see Figure 14, and flux/gap measurements made. The results of the test are included as Figure 15. In the narrow gap of interest (0.125 and under) there is a noticeable increase in the slope of the curve resulting in a 19.3% flux density improvement at the 0.055 in. gap.

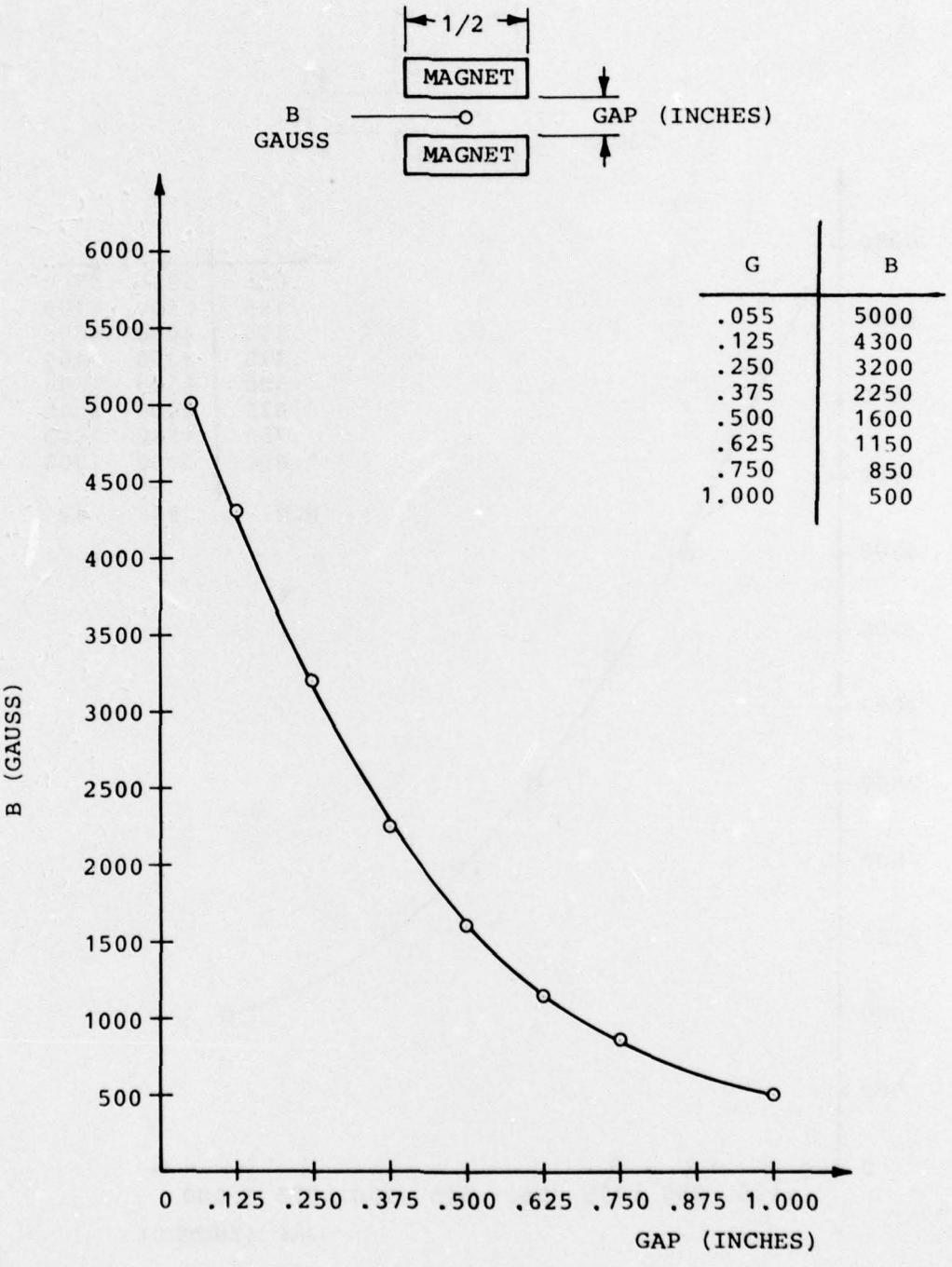

Figure 11. KARS - Flux Density vs Gap SaCo
1/2 Square

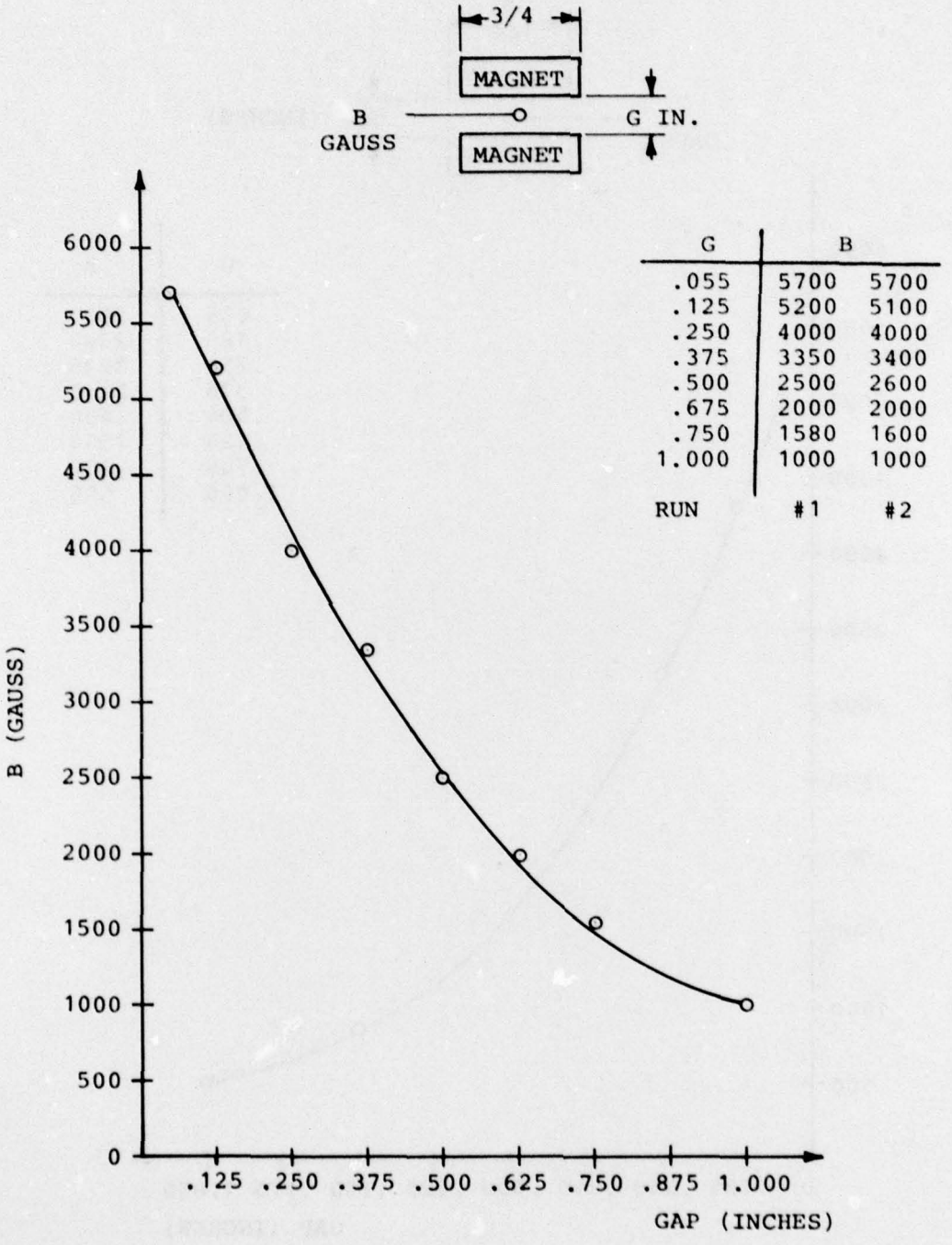

G	B	
.055	5700	5700
.125	5200	5100
.250	4000	4000
.375	3350	3400
.500	2500	2600
.675	2000	2000
.750	1580	1600
1.000	1000	1000
RUN	#1	#2

Figure 12. KARS - Flux Density vs Gap SaCo

3/4 Square

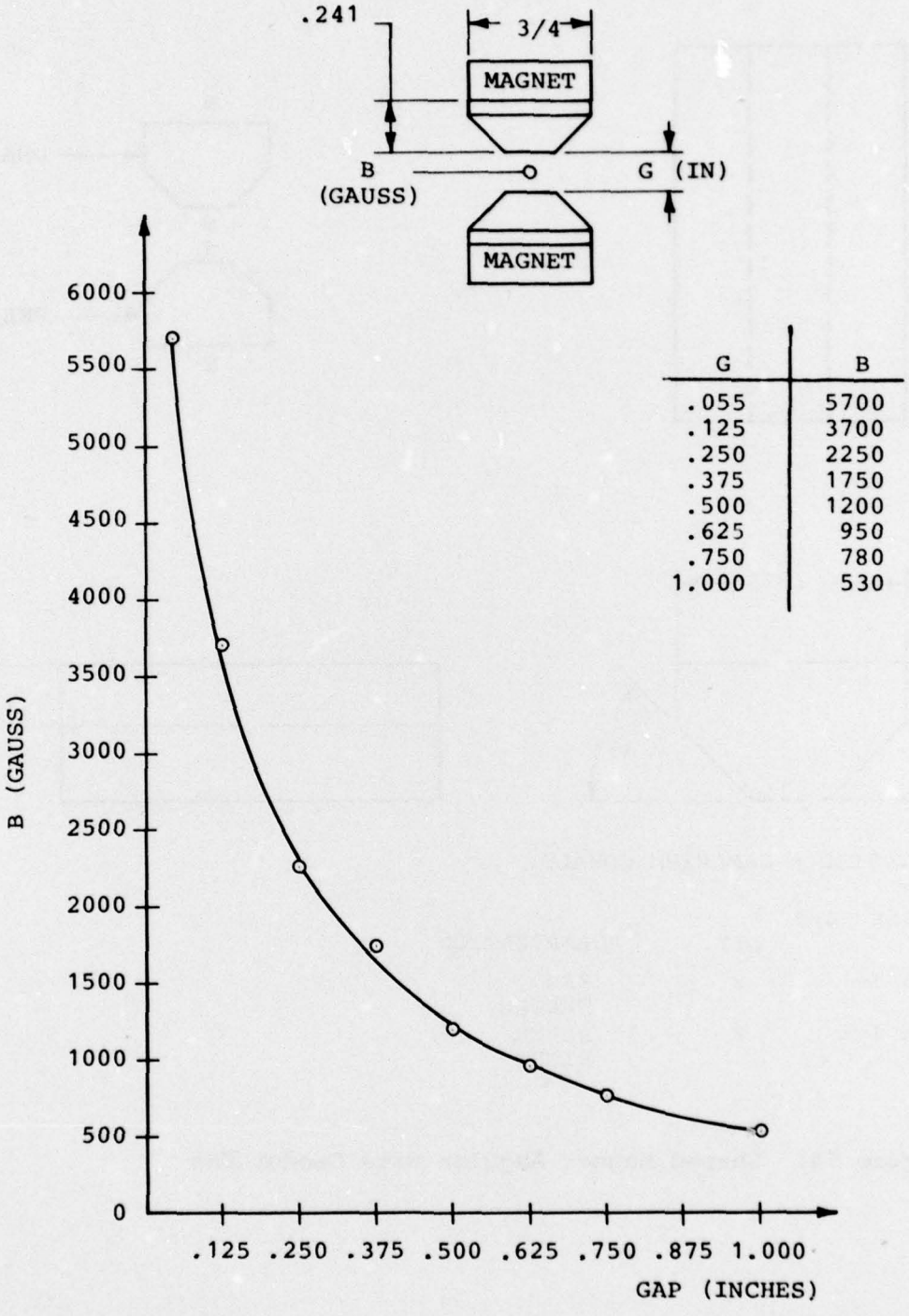

G	B
.055	5700
.125	3700
.250	2250
.375	1750
.500	1200
.625	950
.750	780
1.000	530

Figure 13. Flux Density vs Gap SaCo with Flux Intensifiers

3/4 Square

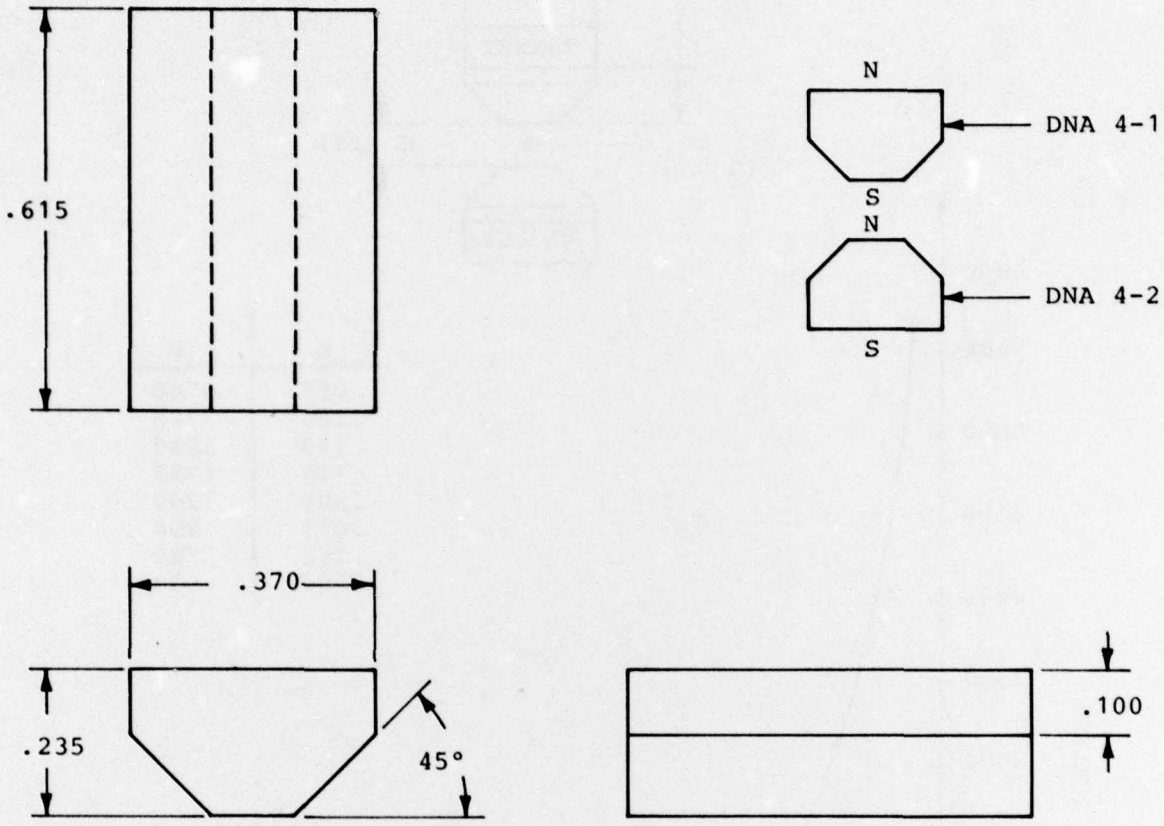

MATERIAL - SAMARIUM COBALT

SCALE 4/1

	QTY.	POLARIZATION
DNA 4-1	2	SEE SKETCH
DNA 4-2	2	UPPER RIGHT

Figure 14. Shaped Magnet Angular Rate Sensor DNA

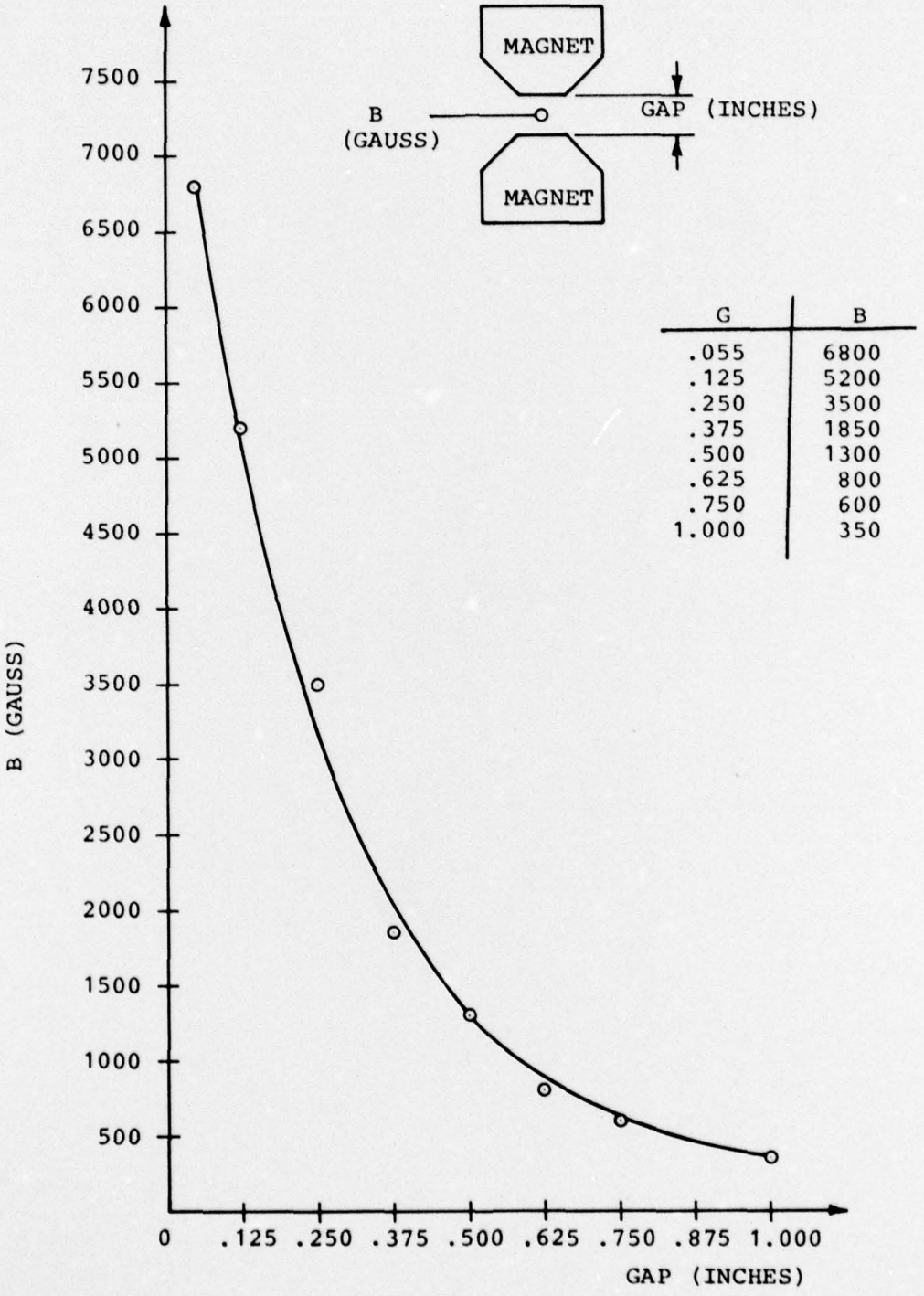

Figure 15. KARS - Flux Density vs Gap Shaped SaCo Magnets

APPENDIX A

PRELIMINARY SPECIFICATION

A.1 SCOPE

A.1.1 General

This specification establishes the requirements identification, manufacture and acceptance of the Kearfott Angular Rate Sensor (KARS), Part No. K (TDB) herein referred to as (KARS).

A.2 APPLICABLE DOCUMENTS

The following documents, of the latest issue in effect, form a part of this specification to the extent specified herein.

Drawings

Kearfott Division

K (TBD)	Rate Sensor, Angular Kearfott
Y (TBD)	Schematic Diagram Wiring

A.3 REQUIREMENTS

A.3.1 Item Definition

The KARS is a damped angular accelerometer, and comprises a conductive liquid annulus (mercury) positioned in the gap of a permanent magnet. The conductive liquid is held in a disk-shaped insulative housing. Upon application of an angular input to the housing, the liquid annulus is coerced into motion by viscous forces. The relative motion of the liquid to the case is sensed by measurement of the potential generated in the liquid as it cuts the lines of force of the permanent magnet. The output potential is amplified to a suitable level by a preamplifier filter assembly.

A.3.1.1 KARS Orientation - The KARS input axis is defined in Figure 1.

A.3.1.2 KARS Mounting Plane - The KARS mounting plane is identified in SKD drawing #K. (TBD)

A.3.2 General Requirements

A.3.2.1 Definitions - The following document defines terminology used in this specification: Aerospace Industries Association, Standard Accelerometer Terminology, EETC Report 30 June 1965.

A.3.3 Performance

The performance specified for all parameters of the KARS are stated as a design goal. An actual performance value, not meeting the requirements stated, shall not be considered in conflict with contractual requirements. The device shall be expected to be useable in two distinctly different regimes known as condition A and condition B. The difference between the two regimes manifests itself in the sensor as changes in the characteristics of the electronics package. It is desirable that the KARS electronics be capable of being set into a configuration appropriate to either mode with a simple switch setting or moving busses.

A.3.3.1 Maximum Input Rate - The KARS shall perform over a maximum input rate of either 10°/sec for condition A, 0r 3000°/sec required, 30,000°/sec desired for condition B.

A.3.3.2 Resolution - The KARS shall perform with a minimum resolution of 2% of full scale.

A.3.3.3 Bandwidth - The KARS shall operate over a bandwidth of 500 Hz for condition A or 5000 Hz desired and 2000 Hz required for condition B.

A.3.3.4 Gain/Scale Factor - The KARS shall have an output of 5 volts for an input of 10°/sec for condition A or 5 volts for an input of 30,000°/sec desired 3000°/sec required for condition B.

A.3.3.5 Corner Frequency - The KARS shall have a corner frequency less than 1 Hz.

A.3.3.6 Rate/Acceleration Contamination - The KARS will have a small component, at very low frequencies, which is proportional to angular acceleration instead of rate. The transfer function for the unit is defined below.

$$Co = \frac{K\ \ddot{\theta}}{1+\tau S}$$

Co = Output voltage before electrical gain

K/τ = Gain factor

A.3.4 Input/Output Requirements

A.3.4.1 Supply Voltage - The KARS shall require a supply voltage of ±6V nominal ±1/2 Volt. Noise ripple shall be less than .05 VP-P.

A.3.4.2 Output Signal Level - The KARS shall have an output level of 5 volts for maximum input.

A.3.5 Mechanical Requirements

A.3.5.1 Exterior Surfaces - All exterior surfaces shall withstand the environment herein specified and the handling expected in the normal course of operation, testing, and maintenance without deterioration which causes non conformance to this specification.

A.3.5.2 Dimensions - The outline, mounting dimensions and location of the center of gravity shall conform to K.

A.3.5.3 KARS Axis - The input axis and its positive direction shall be defined by external markings and by reference mounting surface as indicated by Figure 1.

A.3.5.4 Weight - The weight shall be TBD grams maximum.

A.3.6 Environmental Requirements

The environmental conditions listed in this section are those to which the KARS may be subjected during storage, transportation, and handling or operation, or both. The KARS shall be designed to survive these environments and to successfully complete the environmental tests specified in Section 4.

A.3.6.1 Non Operative Environment - The following conditions, occuring separately or in combination may be encountered during transportation and handling, or storage, or both. The KARS shall conform to all requirements of 3.3 after exposure to any reasonable combinations of the specified service conditions.

A.3.6.1.1 Temperature and Thermal Radiation - Ambient temperature may vary from a minimum of -35°C to a maximum of 71°C under unsheltered ground conditions. Areas exposed to direct sunlight shall be considered as unsheltered conditions.

A.3.6.1.2 Thermal Shock - -35°C to 71°C. The heating and cooling rates of the ambient environment shall be approximately 20°C/sec.

A.3.6.1.3 Vibration - Per Mil Standard 810C Method 514 Figure 514.2-6 curve AB for a 9 minute logarithmic cycle.

A.3.6.2 Operative Environment - The following conditions, occuring separately, or in combination may be encountered during operation. The KARS shall conform to all the requirements of 3.3 during, unless otherwise specified, and after exposure to any reasonable combination of the specified service conditions.

A.3.6.2.1 Mechanical Shock - The KARS shall be capable of withstanding the shock environment specified of 10,000 g peak in a 3.2 milli sec half sin.

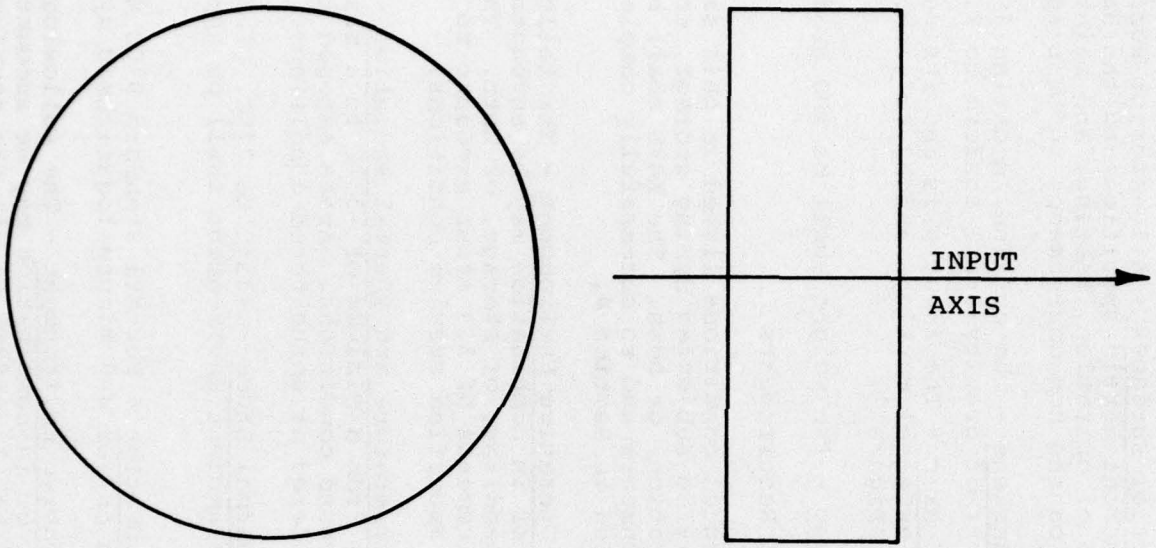

Figure 1. Input Axis Definition

A.3.6.2.2 Temperature - The KARS shall be capable of operating over a temperature range of -29°C to +71°C.

A.3.6.2.3 Magnetic Fields - The KARS shall be capable of withstanding magnetic fields of ±TBD gauss without any degradation of performance.

A.4 QUALITY ASSURANCE

All tests governed by this specification shall be conducted in accordance with test procedures prepared by the contractor.

A.4.1 Classification of Tests

The inspection and testing of the KARS shall be classified as follows.

(1) Acceptance Tests. Acceptance tests are those performed on KARS's submitted for acceptance under contract.

A.4.2 Acceptance Tests

Acceptance tests shall consist of individual tests.

A.4.2.1 Individual Tests - Each KARS shall be subjected to the following tests.

(1) Examination of Product

(2) Impedance

(3) Scale factor

(4) Input axis misalignment

A.4.3 Data Reduction

The data from the KARS shall be reduced using the technique described in Appendix I.

DISTRIBUTION LIST

DEPARTMENT OF DEFENSE

Assistant to the Secretary of Defense
Atomic Energy
ATTN: ATSD (AE)

Director
Defense Advanced Rsch. Proj. Agency
ATTN: Technical Library
ATTN: NMRO
ATTN: PMO
ATTN: STO

Defense Documentation Center
Cameron Station
12 cy ATTN: TC

Director
Defense Nuclear Agency
ATTN: DDST
ATTN: TISI
ATTN: SPTD
ATTN: SPAS
2 cy ATTN: SPSS
3 cy ATTN: TITL

Commander
Field Command, Defense Nuclear Agency
ATTN: FCT
ATTN: FCPR

Chief
Livermore Division, Fld. Command, DNA
Lawrence Livermore Laboratory
ATTN: FCPRL

Chairman
Dept. of Defense Explosives Safety Board
ATTN: T. Zaker

Under Sec'y of Defense for Rsch. & Engrg.
ATTN: S&SS (OS)

DEPARTMENT OF THE ARMY

Dep. Chief of Staff for Rsch. Dev. & Acq.
ATTN: Technical Library

Commander
Harry Diamond Laboratories
ATTN: DELHD-NP
ATTN: DELHD-TI, Technical Library

Director
U.S. Army Engr. Waterways Exper. Sta.
ATTN: W. Flathau
ATTN: F. Hanes
ATTN: J. Ingram

Chief of Engineers
ATTN: DAEN-MCE-D
ATTN: DAEN-RDL
ATTN: DAEN-ASI-L
2 cy ATTN: DAEN-RDM

Commandant, U.S. Army Engineer School
ATTN: ATSEN-SY-L

DEPARTMENT OF THE ARMY (Continued)

Division Engineer
U.S. Army Engineer Div. Ohio River
ATTN: Technical Library

DEPARTMENT OF THE NAVY

Officer-in-Charge
Civil Engineering Laboratory
ATTN: R. Odello
ATTN: Technical Library

Officer-in-Charge
Naval Surface Weapons Center
ATTN: Code WA501, Navy Nuc. Prgms. Off.
ATTN: Code 730, Technical Library

Commanding Officer
Naval Weapons Evaluation Facility
ATTN: R. Hughes
ATTN: Technical Library

DEPARTMENT OF THE AIR FORCE

AF Weapons Laboratory, AFSC
ATTN: DED-I
ATTN: DES-S
ATTN: SUL
ATTN: DE
ATTN: DES-G

Commander
Armament Development & Test Center
ATTN: Technical Library

SAMSO/MN
ATTN: MNN
ATTN: MNNH
ATTN: NMI

DEPARTMENT OF ENERGY

University of California
Lawrence Livermore Laboratory
ATTN: Doc. Con. for Tech. Info. Dept.

Los Alamos Scientific Laboratory
ATTN: Doc. Con. for Technical Library

Sandia Laboratories
Livermore Laboratory
ATTN: Doc. Con. for Technical Library

Sandia Laboratory
ATTN: Doc. Con. for L. Vortman

OTHER GOVERNMENT AGENCY

National Bureau of Standards
ATTN: P. Lederer

DEPARTMENT OF DEFENSE CONTRACTORS

Aerospace Corp.
ATTN: Tech. Info. Services

DEPARTMENT OF DEFENSE CONTRACTORS (Continued)

Agbabian Associates
ATTN: M. Agbabian
ATTN: J. Malthan

EG&G Washington Analytical Services Center, Inc.
ATTN: Technical Library

Boeing Company
ATTN: Technical Library

California Research & Technology, Inc.
ATTN: Technical Library

Electromechanical Sys. of New Mexico, Inc.
ATTN: R. Shunk

General Electric Co.-TEMPO
Center for Advanced Studies
ATTN: DASIAC

H-Tech Laboratories, Inc.
ATTN: B. Hartenbaum

Kaman Sciences Corp.
ATTN: Library

Physics International Co.
ATTN: Doc. Con. for F. Sauer/C. Godfrey
ATTN: Doc. Con. for C. Vincent
ATTN: Doc. Con. for Technical Library

R&D Associates
ATTN: Technical Library
ATTN: C. Knowles

DEPARTMENT OF DEFENSE CONTRACTORS (Continued)

Science Applications, Inc.
ATTN: J. Bratton

SRI International
ATTN: G. Abrahamson
ATTN: D. Keough
ATTN: Technical Library

Systems, Science & Software, Inc.
ATTN: D. Grine
ATTN: Technical Library

TRW Defense & Space Sys. Group
ATTN: Tech. Info. Center/S-1930
2 cy ATTN: P. Lieberman

Terra Tek, Inc.
ATTN: S. Green
ATTN: Technical Library

The Eric H. Wang
Civil Engineering Rsch. Fac.
ATTN: Library

The Singer Company
Kearfatt Division
2 cy ATTN: J. Evans
2 cy ATTN: R. Weber